ATTACHMENT 10

Westinghouse Letter LTR-SGMP-09-100 NP-Attachment, "Response to NRC Request for Additional Information on H*; Model F and Model D5 Steam Generators" (questions 1 through 20 and 24 of the NRC RAI) (Non-Proprietary)

Westinghouse Electric Company

# Response to NRC Request for Additional Information on H*; Model F and Model D5 Steam Generators

August 12, 2009

Westinghouse Electric Company LLC
P.O. Box 158
Madison, PA 15663

© 2009 Westinghouse Electric Company LLC
All Rights Reserved

**Response to**
**NRC Request for Additional Information on H*;**
**Model F and Model D5 Steam Generators**

**References:**


1. NL-09-0547, Vogtle Electric Generating Plant License Amendment Request to Revise Technical Specification(TS) Sections 5.5.9, "Steam Generator (SG) Program" and TS 5.6.10, "Steam Generator Tube Inspection Report for Permanent Alternate Repair Criteria," Southern Company, May 19, 2009.

2. RS-09-071, " License Amendment Request to Revise Technical Specifications (TS) for Permanent Alternate Repair Criteria," Exelon Nuclear, June 24, 2009.

3. CP-200900748, Log # TXX-09075, "Comanche Peak Steam Electric Station (CPSES) Docket Nos. 50-445 and 50-446, License Amendment Request 09-007, Model D5 Steam Generator Alternate Repair Criteria," Luminant, June 8, 2009.

4. SBK-L-09118, "Seabrook Station: License Amendment Request 09-03; Revision to Technical Specification 6.7.6.k, "Steam Generator (SG) Program," for Permanent Alternate Repair Criteria (H*)," May 28, 2009.

5. Vogtle Electric Generating Plant, Units 1 and 2, Request for Additional Information Regarding Steam Generator Program (TAC Nos. ME1339 and ME1340)," United States Nuclear Regulatory Commission, July 10, 2009.

6. Braidwood Station, Units 1 and 2, and Byron Station, Unit Nos. 1 and 2 – Request for Additional Information Related to Steam Generator Permanent Alternate Repair Criteria (TAC Nos. ME1613, ME1614, ME1615, and ME1616)," United States Nuclear Regulatory Commission, July 20, 2009.

7. Comanche Peak Steam Electric Station, Units 1 and 2 – Request for Additional Information Regarding the Permanent Alternate Repair Criteria License Amendment Request (TAC Nos. ME1446 and ME1447)," United States Nuclear Regulatory Commission, July 23, 2009.

8. WCAP-17071-P, "H*: Alternate Repair Criteria for the Tubesheet Expansion Region in Steam Generators with Hydraulically Expanded Tubes (Model F)," Westinghouse Electric LLC, April 2009.

9. WCAP-17072-P, "H*: Alternate Repair Criteria for the Tubesheet Expansion Region in Steam Generators with Hydraulically Expanded Tubes (Model D5)," Westinghouse Electric LLC, May 2009.

10. "Vogtle Electric Generating Plant, Units 1 and 2, Request for Additional Information Regarding Steam Generator Program (TAC Nos. ME1339 and ME1340)," United States Nuclear Regulatory Commission, August 5, 2009

**Introduction**

In response to formal requests for technical specification amendments, References 1, 2, 3 and 4, the USNRC formally requested additional information in References 5, 6 and 7. A preliminary request was received in response to Reference 4. This document provides responses to NRC RAI on the Vogtle, Byron/Braidwood and Comanche Peak requests for a permanent license amendment to implement H*. These plants represent the Model F and Model D5 steam generators for which the H* technical justification is provided in Reference 8 and 9. It is anticipated that similar RAIs may be issued as other LARs are submitted that include other models of SG, specifically Models 44F and 51F. The intent of these responses is to provide a generic response for all applicable models of SGs to the extent possible, recognizing that there may be specific numerical differences for the models of SG not yet addressed (Model 44F and Model 51F). If necessary, a second issue of these responses will be provided to specifically address the Model 44F and Model 51 RAI when they are received.

The NRC questions are repeated verbatim for each of the plants who received formal or draft RAI in the tables preceding the response to each question. The current NRC RAIs are specifically in regard to WCAP-17071-P (Model F H*) and WCAP-17072-P (Model D5 H*); responses are provided primarily for these reports, but additional information is provided as appropriate for the H* reports for the other models of SGs , WCAP-17091-P for the Model 44F and WCAP-17092-P for the Model 51 F. Because the reports all utilize the same methodology, model-specific information provided will generally be different in only the numerical information.

Subsequent to the initial issue of the RAI (References 5, 6 and 7), the NRC issued follow-up questions (Reference 10) to question numbers 4, 20 and 24 and an additional question regarding a TS commitment for applying the leakage factors. The responses to the follow-up questions to original question numbers 20 and 24 are included directly in the response to these questions below. The response to RAI#4 and the follow-up question to RAI#4 will be provided under separate cover.

Where references are made in a response to other responses included in this document, the basis for the reference is the RAI received by Vogtle. For example, the Vogtle RAI#20 response applies to the Byron/Braidwood RAI#21 as noted in the tabularization of the questions preceding each response.

| | | |
|---|---|---|
| ***RAI*** | *Vogtle* | *1. Reference 1, page 6-21, Table 6-6: This table contains a number of undefined parameters and some apparent inconsistencies with Table 5-2 on page 5-6. Please define the input parameters in Table 6-6.* |
| | *WCGS* | *1. Reference 1, page 6-21, Table 6-6: This table contains a number of undefined parameters and some apparent inconsistencies with Table 5-2 on page 5-6. Please define the input parameters in Table 6-6.* |
| | *B/B* | *1. Reference 1, Page 6-21, Table 6-6: This table contains a number of undefined parameters and some apparent inconsistencies with Table 5-2 on page 5-6. Please define the input parameters in Table 6-6.* |
| | *CPSES* | *1. Reference 1, page 6-21, Table 6-6: This table contains a number of undefined parameters and some apparent inconsistencies with Table 5-2 on page 5-6. Please define the input parameters in Table 6-6.* |
| | *Seabrook* | *1. Reference 1, Page 6-21, Table 6-6: This table contains a number of undefined parameters and some apparent inconsistencies with Table 5-2 on page 5-6. Please define the input parameters in Table 6-6.* |

Response:

Table 6-6 in WCAP-17071-P and WCAP-17072-P is provided principally as a reference to provide a bridge to the source of basic design data maintained by Westinghouse and as a historical reference from prior H* reports. Although many of the entries in Table 6-6 are not used in the H* analysis, the table was provided to show traceability to the principal sources of the design data, the Westinghouse Power Capability Working Group (PCWG) sheets and the Systems Standards 1.3F and 1.3, which provide transient response data for component design. The references to Millstone Unit 3 in WCAP-17071-P and to Byron Unit 2 in WCAP-17072-P reflect that these plants are the limiting plants for the Model F and Model D5 SGs that are candidates for application of H*.

Updated Tables 6-6 for the Model F and Model D5 are provided as Tables RAI1-2 and RAI1-3. The references in the tables have been updated from those contained in Revision 0 of WCAP-17071-P and WCAP-17072-P.

**Table RAI1-1**
**Updated Table 6-6 of WCAP-17071-P: Summary of H* Millstone Unit 3 Analysis**
**Mean Input Properties**

| | |
|---|---|
| **Plant Name** | Millstone Unit 3 |
| **Plant Alpha** | NEU |
| **Plant Analysis Type** | Hot Leg |
| **SG Type** | F |

| **Input** | **Value** | **Unit** | **Reference** |
|---|---|---|---|
| **Accident and Normal Temperature Inputs** | | | |
| NOP $T_{hot}$ | | °F | PCWG-06-9 |
| NOP $T_{low}$ | | °F | PCWG-06-9 |
| SLB TS ΔT | | °F | 1.3F |
| SLB CH ΔT | | °F | 1.3F |
| Shell ΔT | | °F | 1.3F |
| FLB Primary ΔT Hi | | °F | 1.3F |
| FLB Primary ΔT Low | | °F | 1.3F |
| SLB Primary ΔT | | °F | 1.3F |
| SLB Secondary ΔT | | °F | 1.3F |
| Secondary Shell ΔT Hi | | °F | PCWG-06-9 |
| Secondary Shell ΔT Low | | °F | PCWG-06-9 |
| Cold Leg ΔT | | °F | PCWG-06-9 |
| Hot Standby Temperature | | °F | PCWG-06-9 |
| **Operating Pressure Input** | | | |
| Faulted SLB Primary Pressure | 2560.0 | psig | 1.3F |
| Faulted FLB Primary Pressure | 2642.0(1) | psig | 1.3F |
| Normal Primary Pressure | 2235.0 | psig | PCWG-06-9 |
| Cold Leg ΔP | | psig | NSD-RMW-90-070 |
| NOP Secondary Pressure – Low | | psig | PCWG-06-9 |
| NOP Secondary Pressure – Hi | | psig | PCWG-06-9 |
| Faulted FLB Secondary Pressure | 0.0 | psig | 1.3F |
| Faulted SLB Secondary Pressure | 0.0 | psig | 1.3F |

a,c,e

Notes. 1. The value for Faulted FLB Primary Pressure used in the H* analysis is 2650 psi which conservatively bounds the limiting value of 2642 psi as identified in SSDC 1.3F for the Model F SGs. The value of 2642 psig for peak primary-secondary pressure differential differs from the value provided in Table 5-3 (2657 psig) reported in WCAP-17071-P.

**Table RAI1-2**
**Updated Table 6-6 of WCAP-17072-P: Summary of H* Byron Unit 2 Analysis**
**Mean Input Properties**

| | |
|---|---|
| **Plant Name** | Byron 2 |
| **Plant Alpha** | CBE |
| **Plant Analysis Type** | Hot Leg |
| **SG Type** | D5 |

| **Input** | **Value** | **Unit** | **Reference** |
|---|---|---|---|
| **Accident and Normal Temperature Inputs** | | | |
| | | a,c,e | |
| NOP $T_{hot}$ | | °F | PCWG-2741 |
| NOP $T_{low}$ | | °F | PCWG-2741 |
| SLB TS ΔT | | °F | 1.3, Rev. 2 |
| SLB CH ΔT | | °F | 1.3, Rev. 2 |
| Shell ΔT | | °F | 1.3, Rev. 2 |
| FLB Primary ΔT | | °F | 1.3, Rev. 2 |
| SLB Primary ΔT | | °F | 1.3, Rev. 2 |
| SLB Secondary ΔT | | °F | 1.3, Rev. 2 |
| Secondary Shell ΔT Hi | | °F | PCWG-2741 |
| Secondary Shell ΔT Low | | °F | PCWG-2741 |
| Cold Leg ΔT | | °F | PCWG-2741 |
| Hot Standby Temperature* | | °F | PCWG-2741 |
| **Operating Pressure Input** | | | |
| Faulted SLB Primary Pressure | 2560.0 | psig | 1.3, Rev. 2 |
| Faulted FLB Primary Pressure | 2560.0 | psig | 1.3, Rev. 2 |
| Normal Primary Pressure | 2235.0 | psig | PCWG-2741 |
| Cold Leg ΔP | | a,c,e psig | NSD-RMW-90-070 |
| NOP Secondary Pressure – Low | | psig | PCWG-2741 |
| NOP Secondary Pressure – Hi | | psig | PCWG-2741 |
| Faulted FLB Secondary Pressure | 0.0 | psig | 1.3, Rev. 2 |
| Faulted SLB Secondary Pressure | 0.0 | psig | 1.3, Rev. 2 |

Much of the data provided in Table 6-6 is not utilized in the final H* analysis. Table RAI1-3 provides a summary of whether the data is utilized in the reference analysis of H* and in which analysis model it is used (See Figure 1-1 in the respective reports). <u>It is emphasized that changes made in Tables RAI1-1 and RAI1-2 do not affect the H* results provided in References 7 and 8 of this document.</u>

**Table RAI1-3**
**Utilization of Data from Table 6-6**

| Input | Where Used |
|---|---|
| **Accident and Normal Temperature Inputs** | |
| NOP $T_{hot}$ | H* Integrator Spreadsheet |
| NOP $T_{low}$ | H* Integrator Spreadsheet |
| SLB TS $\Delta T$ | Not Used |
| SLB CH $\Delta T$ | Not Used |
| Shell $\Delta T$ | Not Used |
| FLB Primary $\Delta T$ Hi | Not Used |
| FLB Primary $\Delta T$ Low | Not Used |
| SLB Primary $\Delta T$ | Not Used |
| SLB Secondary $\Delta T$ | Not Used |
| Secondary Shell $\Delta T$ Hi | H* Integrator Spreadsheet; same as Secondary Fluid Temperature at NOP High $T_{avg}$ Conditions |
| Secondary Shell $\Delta T$ Low | H* Integrator Spreadsheet; same as Secondary Fluid Temperature at NOP Low $T_{avg}$ Conditions |
| Cold Leg $\Delta T$ | Not Used |
| Hot Standby Temperature | H* Integrator Spreadsheet |
| **Operating Pressure Input** | |
| Faulted SLB Primary Pressure | H* Integrator Spreadsheet |
| Faulted FLB Primary Pressure | H* Integrator Spreadsheet |
| Normal Primary Pressure | H* Integrator Spreadsheet |
| Cold Leg $\Delta P$ | Not Used |
| NOP Secondary Pressure – Low | H* Integrator Spreadsheet |
| NOP Secondary Pressure – Hi | H* Integrator Spreadsheet |
| Faulted FLB Secondary Pressure | Not Used |
| Faulted SLB Secondary Pressure | Not Used |
| | |

The definitions of the entries in the Table 6-6 of WCAP-17071-P and WCAP17072-P are presented below. Also, discussion is provided regarding the consistency of the values in Table 6-6 of the respective reports with Tables 5-1 through 5-6 of the reports.

**NOP $T_{hot}$**

The steam generator hot leg temperature at high $T_{avg}$ normal operating conditions at 100% power (considered to be the same as the reactor vessel outlet temperature).

Model F: [ ]$^{a,c,e}$ °F at the inlet of the tubes at high $T_{avg}$ normal operating conditions at 100% power for Millstone Unit 3 is consistent with the value provided in Table 5-1 (WCAP-17071-P).

Model D5: [ ]$^{a,c,e}$ °F at the inlet of the tubes at high $T_{avg}$ normal operating conditions at 100% power Byron Unit 2 is consistent with the value provided in Table 5-1 (WCAP-17072-P).

**NOP $T_{low}$**

The steam generator hot leg temperature at the inlet of the tubes at low $T_{avg}$ normal operating conditions at 100% power (considered to be the same as the reactor vessel outlet temperature).

Model F: [ ]$^{a,c,e}$ °F is consistent with the value provided in Table 5-1.

Model D5: [ ]$^{a,c,e}$ °F is consistent with the value provided in Table 5-1.

**SLB TS ΔT**

Model F: [ ]$^{a,c,e}$ °F, ([ ]$^{a,c,e}$ °F - 70°F )= [ ]$^{a,c,e}$ °F: The steam generator hot and cold leg temperature difference that occurs during a postulated steam line break event during the maximum pressure difference across the tubesheet of 2560 psi between the steady-state tubesheet metal temperature and the ambient temperature surrounding the steam generator (assumed to be 70°F). The value of [ ]$^{a,c,e}$ °F is not used in the analysis.

Model D5: [ ]$^{a,c,e}$ °F , ([ ]$^{a,c,e}$ °F - 70°F)= [ ]$^{a,c,e}$ °F: The steam generator hot and cold leg temperature difference that occurs during a postulated steam line break event during the maximum pressure difference across the tubesheet of 2560 psi between the steady-state tubesheet metal temperature and the ambient temperature surrounding the steam generator (assumed to be 70°F). The value of [ ]$^{a,c,e}$ °F is not used in the H* analysis.

**SLB CH ΔT-**

Model F: 348°F, [ ]$^{a,c,e}$ °F: The steam generator hot and cold leg temperature difference that occurs during a postulated steam line break event during the maximum pressure difference across the tubesheet of 2560 psi between the steady-state channelhead metal temperature and the ambient temperature surrounding the steam generator (assumed to be 70°F). The value of [ ]$^{a,c,e}$ °F is not used in the H* analysis.

Model D5: 227°F, ([ ]$^{a,c,e}$ °F: The steam generator hot and cold leg temperature difference that occurs during a postulated steam line break event during the maximum pressure difference across the tubesheet of 2560 psi between the steady-state channelhead metal temperature and the ambient temperature surrounding the steam generator (assumed to be 70°F). The value of [ ]$^{a,c,e}$ °F is not used in the H* analysis.

**Shell ΔT**

Model F: ([ ]$^{a,c,e}$ °F -70°F) = [ ]$^{a,c,e}$ °F : The steam generator secondary side temperature difference that occurs during a postulated steam line break event during the maximum pressure difference across the tubesheet of 2560 psi between the steady-state secondary side shell metal temperature and the ambient temperature surrounding the steam generator (assumed to be 70°F). The [ ]$^{a,c,e}$ °F value is not used in the H* analysis.

Model D5: [ ]$^{a,c,e}$ °F. The steam generator secondary side temperature difference that occurs during a postulated steam line break event during the maximum pressure difference across the tubesheet of 2560 psi between the steady-state secondary side shell metal temperature and the ambient temperature surrounding the steam generator (assumed to be 70°F). The [ ]$^{a,c,e}$ °F value is not used in the H* analysis.

The secondary side temperature during a postulated SLB is used in the H* analysis for both the Model F ([ ]$^{a,c,e}$ °F) and Model D5 ([ ]$^{a,c,e}$ °F) SGs.

**FLB Primary $\Delta T_{Hi}$**

The reduction in NOP $T_{hot}$ temperature that occurs during a postulated feedwater line break during the maximum pressure difference across the tubesheet of 2642 psi (Model F), 2560 psi (Model D5) corresponding to the high $T_{avg}$ plant condition.

Model F: [ ]$^{a,c,e}$ °F is consistent with the value provided in Table 5-3 ([ ]$^{a,c,e}$ °F- 54°F = [ ]$^{a,c,e}$ °F). The - 54°F value is not used in the H* analysis.

Model D5: [ ]$^{a,c,e}$ °F is consistent with the value provided in Table 5-3 ([ ]$^{a,c,e}$ °F)- [ ]$^{a,c,e}$ °F = [ ]$^{a,c,e}$ °F). The [ ]$^{a,c,e}$ °F value is not used in the H* analysis.

The primary side temperature that occurs during a postulated FLB initiating from the high $T_{avg}$ plant condition, [ ]$^{a,c,e}$ °F is used in the H* analysis for the Model F SG. The no load temperature of [ ]$^{a,c,e}$ °F is used for the Model D5 SGs.

**FLB Primary $\Delta T_{Low}$**

The reduction in NOP $T_{low}$ temperature that occurs during a postulated feedwater line break during the maximum pressure difference across the tubesheet of 2642 psi.

Model F: [ ]$^{a,c,e}$ °F is consistent with the value provided in Table 5-3 ([ ]$^{a,c,e}$ °F [ ]$^{a,c,e}$ °F = [ ]$^{a,c,e}$ °F). The -54°F value is not used in the H* analysis.

Model D5: [ ]$^{a,c,e}$ °F is not included in WCAP-17072-P. The [ ]$^{a,c,e}$ °F value is not used in the H* analysis.

The primary side temperature that occurs during a postulated FLB initiating from the low $T_{avg}$ plant condition, [ ]$^{a,c,e}$ °F, is used in the H* analysis for the Model F. The no load temperature of [ ]$^{a,c,e}$ °F is used for the Model D5 SGs.

**SLB Primary ΔT**

Model F: The reduction in no load temperature of [ ]$^{a,c,e}$ °F [ ]$^{a,c,e}$ °F) to [ ]$^{a,c,e}$ °F that occurs in the reactor coolant system during a postulated SLB during the maximum pressure difference across the tubesheet of 2560 psi. The value in Table 6-6 should be [ ]$^{a,c,e}$ °F to be consistent with SSDC 1.3F and Table 5-2. The [ ]$^{a,c,e}$ °F value is not used in the H* analysis.

Model D5: The reduction in no load temperature of [ ]$^{a,c,e}$ °F ([ ]$^{a,c,e}$ °F) to [ ]$^{a,c,e}$ °F that occurs in the reactor coolant system during a postulated SLB during the maximum pressure difference across the tubesheet of 2560 psi. The value in Table 6-6 is consistent with SSDC 1.3, Rev 2 and Table 5-2. The [ ]$^{a,c,e}$ °F value is not used in the H* analysis.

The primary side temperature that occurs during a postulated SLB, [ ]$^{a,c,e}$ °F, is used in the H* analysis for the Model F. The primary side temperature, [ ]$^{a,c,e}$ °F, is used for the Model D5 SGs.

**SLB Secondary ΔT**

Model F: The reduction in no load temperature of [ ]$^{a,c,e}$ °F ([ ]$^{a,c,e}$ °F) to [ ]$^{a,c,e}$ °F that occurs on the secondary side of the steam generator during a postulated SLB during the maximum pressure difference across the tubesheet of 2560 psi. The value in Table 6-6 should be [ ]$^{a,c,e}$ °F to be consistent with Table 5-2.

Model D5: The reduction in no load temperature of [ ]$^{a,c,e}$ °F ([ ]$^{a,c,e}$ °F) to [ ]$^{a,c,e}$ °F that occurs on the secondary side of the steam generator during a postulated SLB during the maximum pressure difference across the tubesheet of 2560 psi. The value in Table 6-6 should be [ ]$^{a,c,e}$ °F to be consistent with SSDC 1.3, Rev. 2 and Table 5-2.

As noted above, the secondary side temperature during a postulated SLB is used in the H* analysis for both the Model F ([ ]$^{a,c,e}$ °F) and Model D5 ([ ]$^{a,c,e}$ °F) SGs.

**Secondary Shell $\Delta T_{Hi}$**

For the Model F SG, [ ]$^{a,c,e}$ °F (should be [ ]$^{a,c,e}$ °F) is the average temperature between the secondary side steam temperature and the feedwater temperature during NOP Hi $T_{avg}$ operation ([ ]$^{a,c,e}$ °F + [ ]$^{a,c,e}$ °F). This value is the same as the secondary fluid temperature during high $T_{avg}$ normal operating conditions. The same value calculated for the Model D5 SGs is [ ]$^{a,c,e}$ °F.

**Secondary Shell $\Delta T_{Low}$**

For the Model F SGs, [ ]$^{a,c,e}$ °F is the average temperature between the secondary side steam temperature and the feedwater temperature during NOP Low $T_{avg}$ operation ([ ]$^{a,c,e}$ °F + [ ]$^{a,c,e}$ °F)/2= [ ]$^{a,c,e}$ °F). This value is the same as the secondary fluid temperature during low $T_{avg}$ normal operating conditions. The same value calculated for the Model D5 SGs is [ ]$^{a,c,e}$ °F.

**Cold Leg $\Delta T$**

Model F: The temperature difference between the hot and cold leg of the Millstone 3 SGs during NOP Low $T_{avg}$ is 66.6°F. This value is not used in the H* analysis.

Model D5: The temperature difference between the hot and cold leg of the Byron 2/Braidwood 2 SGs during NOP Low $T_{avg}$ is 63°F. This value is not used in the H* analysis.

**Hot Standby Temperature**

The zero load temperature, [ ]$^{a,c,e}$ °F.

This value is used in the H* analysis for both the Model F and Model D5 SGs.

**Faulted SLB Primary Pressure**

The maximum pressure difference that occurs across the tubesheet during a postulated SLB.

Model F: 2560 psig is consistent with the value reported in Table 5-2.

Model D5: 2560 psig is consistent with the value reported in Table 5-2.

**Faulted FLB Primary Pressure**

The maximum pressure difference that occurs across the tubesheet during a postulated FLB.

Model F: The value (2650 psig) used for the Model F SG in the H* analysis bounds the actual FLB pressure differential, 2642 psi identified in SSDC 1.3F. As noted above, Table 5-3 of

WCAP-17071-P should be corrected to 2642 psig for the entries for peak primary-to-secondary pressure.

Model D5: The maximum FLB pressure differential for the Model D5 SGs is 2560 psi.

**Normal Primary Pressure**

The primary side pressure during normal operation.

Model F: 2235 psig is consistent with the absolute primary pressure reported in Table 5-1 of 2250 psia.

Model D5: 2235 psig is consistent with the absolute primary pressure reported in Table 5-1 of 2250 psia.

**Cold Leg ΔP**

The overall pressure drop that occurs in a steam generator tube as fluid flows through the tube from hot leg to cold leg.

Model F: [ ]$^{a,c,e}$ psig (Millstone 3). This value is not used in the H* analysis.

Model D5: [ ]$^{a,c,e}$ psig (Byron 2/Braidwood 2). This value is not used in the H* analysis.

**NOP Secondary Pressure Low**

The steam pressure on the secondary side of the steam generators for NOP Low $T_{avg}$.

Model F: [ ]$^{a,c,e}$ psig is consistent with the value reported in Table 5-1 as [ ]$^{a,c,e}$ psia.

Model D5: [ ]$^{a,c,e}$ psig is consistent with the value reported in Table 5-1 as [ ]$^{a,c,e}$ psia.

**NOP Secondary Pressure Hi**

The steam pressure on the secondary side of the steam generators for NOP Hi $T_{avg}$.

Model F: [ ]$^{a,c,e}$ psig is consistent with the value reported in Table 5-1 as [ ]$^{a,c,e}$ psia.

Model D5: [ ]$^{a,c,e}$ psig is consistent with the value reported in Table 5-1 as [ ]$^{a,c,e}$ psia.

**Faulted FLB Secondary Pressure**

0 psig, for the Model F and Model D5 SGs, the steam pressure on the secondary side of a steam generator during a postulated FLB. This value is not used in the H* analysis.

| | | |
|---|---|---|
| ***RAI*** | *Vogtle* | 2. *Reference 1, page 6-23, Section 6.2.2.2: Why was the finite element analysis not run directly with the modified temperature distribution rather than running with the linear distribution and scaling the results?* |
| | *WCGS* | 2. *Reference 1, Section 6.2.2.2: Please explain why the finite element analysis not run directly with the modified temperature distribution rather than running with the linear distribution and scaling the results?* |
| | *B/B* | 2. *Reference 1, Section 6.2.2.2: Why was the finite element analysis not run directly with the modified temperature distribution rather than running with the linear distribution and scaling the results?* |
| | *CPSES* | 2. *Reference 1, Section 6.2.2.2: Please explain why the finite element analysis was not run directly with the modified temperature distribution rather than running with the linear distribution and scaling the results?* |
| | *Seabrook* | 2. *Reference 1, Section 6.2.2.2: Why was the FEA analysis not run directly with the modified temperature distribution rather than running with the linear distribution and scaling the results?* |

Response:

The finite element analysis was run with the modified temperature distribution as described in section 6.2.2.2.5 of WCAP 17071-P (Model F) and WCAP-17072-P (Model D5). However, since the modified temperature distribution required a different meshing scheme, the displacement results could not initially be used as inputs to the H* contact pressure analysis. The difficulty in applying the results for the modified temperature distribution is what led to the development of Figures 6-21 through Figure 6-23. Additional tools were developed to accommodate the displacement results from the modified temperature distribution during the course of refining the analysis procedures to accommodate other steam generator designs. When the actual tubesheet displacements from the modified thermal distribution are used, instead of the results from the linear temperature distribution being scaled, the actual change in H* distance is much less than the [ ]$^{a,c,e}$ inches reported in Section 6.2.2.2.5. The value of the adjustment for the thermal distribution effect in H* for the different models of SG in the H* fleet is given in Table RAI2-1. All of the values in Table RAI2-1 assume zero residual contact pressure from tube installation effects. The results in column (3) come from using the scaled linear tubesheet displacements in the H* contact pressure analysis. The results in column (4) come from using the tubesheet displacements from the modified thermal distribution.

**Table RAI2-1**

**Updated NOP Thermal Offset Factors**

| SG Model | Report | Thermal Offset (Scaled Result) | Thermal Offset (Applied) |
|---|---|---|---|
| (1) | (2) | (3) | (4) |
| Model F | WCAP 17071-P | [ ]a,c,e in. | [ ]a,c,e in. |
| Model D5 | WCAP 17072-P | [ ]a,c,e in. | [ ]a,c,e in. |
| Model 44F | WCAP 17091-P | 0.00 in. | 0.00 in. |
| Model 51F | WCAP 17092-P | 0.00 in. | 0.00 in. |

| | | |
|---|---|---|
| ***RAI*** | *Vogtle* | *3. Reference 1, page 6-38, Section 6.2.3: Why is radial displacement the "figure of merit" for determining the bounding segment? Does circumferential displacement not enter into this? Why is the change in the tube hole diameter not the "figure of merit?"* |
| | *WCGS* | *3. Reference 1, Section 6.2.3: Please explain why radial displacement is the "figure of merit" for determining the bounding segment? Does circumferential displacement not enter into this? Why is the change in tube hole diameter not the "figure of merit?"* |
| | *B/B* | *3. Reference 1, Section 6.2.3: Why is radial displacement the "figure of merit" for determining the bounding segment? Does circumferential displacement not enter into this? Why is the change in tube hole diameter not the "figure of merit?"* |
| | *CPSES* | *3. Reference 1, Section 6.2.3: Please explain why radial displacement is the "figure of merit" for determining the bounding segment. Does circumferential displacement not enter into this? Why is the change in tube hole diameter not the "figure of merit?"* |
| | *Seabrook* | *3. Reference 1, Section 6.2.3: Why is radial displacement the "figure of merit" for determining the bounding segment? Does circumferential displacement not enter into this? Why is the change in tube hole diameter not the "figure of merit?"* |

Response:

Radial displacement is calculated in two different ways in the H* analysis: the global scale and the local scale.

On the scale of the steam generator itself, otherwise referred to as the global scale, the radial displacement of the entire tubesheet is calculated. At this level, the tubes are not included in the structural model and there is no direct way to calculate the change in the tube hole diameter. It is not possible to calculate the change in the tube hole diameter at the global scale because the tube holes physically do not exist but are represented by

the effective anisotropic material properties of the tubesheet. Therefore, from the global perspective, it is not possible to use the change in hole diameter as a "figure of merit."

On the local scale, the displacements of the tube and tubesheet collar are calculated in the radial and circumferential directions. As described in Section 6.3 of WCAP-17071-P (Model F) and WCAP -17072-P (Model D5), the expansion of a hole of diameter D in the tubesheet at a radius R is given by:

Radial: $\Delta D = D \{dU_R(R)/dR\}$

Circumferential: $\Delta D = D \{U_R(R)/R\}$

$U_R$ is available directly from the finite element results as the global radial displacement for a given point in the tubesheet. The value for $dU_R(R)/dR$ is obtained by numerical differentiation of the combined displacement field. The maximum expansion of a hole in the tubesheet is in either the radial or circumferential direction. Typically, these two values are within [ ]$^{a,c,e}$% of each other. However, it is clear from the relationship described in Section 6.3 that maximizing the radial displacement at the global scale (i.e., increasing $U_R$) results in maximizing the circumferential and radial displacement of the tubesheet material at the local scale.

The connection between the local and global scales is the global radial displacement of the tubesheet. This is because the applied boundary conditions and the structures attached to the tubesheet have the greatest effect on the displacement in the radial direction. The tubesheet displacement in the circumferential direction due to the applied pressure loading is typically constant at a small negative value on the order of [ ]$^{a,c,e}$ inch or less. Therefore, the radial displacement is the best indicator, or "figure of merit," of the effect of different operating conditions on tubesheet displacement due to pressure loading. Radial displacement is also a good "figure of merit" for the change in tube hole diameter because maximizing the global radial displacement leads to the maximum calculated circumferential and radial tubesheet displacements at the local level. Therefore, the global radial displacement of the tubesheet as described in Section 6.2.3 is the appropriate choice for determining the bounding segment of the tubesheet with respect to the contact pressure analysis.

| | | |
|---|---|---|
| ***RAI*** | *Vogtle* | *4. Reference 1, page 6-69: In Section 6.2.5.3, it is concluded that the tube outside diameter and the tubesheet tube bore inside diameter always maintain contact in the predicted range of tubesheet displacements. However, for tubes with through-wall cracks at the H* distance, there may be little or no net pressure acting on the tube for some distance above H*. In Tables 6-18 and 6-19, the fourth increment in the step that occurs two steps prior to the last step suggests that there may be no contact between the tube and tubesheet, over a portion of the circumference, for a distance above H*. Is the conclusion in Section 6.2.5.3 valid for the entire H* distance, given the possibility that the tubes may contain through-wall cracks at that location?* |
| | *WCGS* | *4. Reference 1, page 6-69: In Section 6.2.5.3, it is concluded that the tube outside diameter and the tubesheet tube bore inside diameter always maintain contact in the predicted range of tubesheet displacements. However, for tubes with through-wall cracks at the H* distance, there may be little or no net pressure acting on the tube for some distance above H*. In Tables 6-18 and 6-19, the fourth increment in the step that occurs two steps prior to the last step suggests that there may be no contact between the tube and tubesheet, over a portion of the circumference, for a distance above H*. Is the conclusion in 6.2.5.3 valid for the entire H* distance, given the possibility that the tubes may contain through-wall cracks at that location?* |
| | *B/B* | *4. Reference 1, Page 6-7: In Section 6.2.5.3, it is concluded that the tube outside diameter and the tubesheet tube bore inside diameter always maintain contact in the predicted range of tubesheet displacements. However, for tubes with through-wall cracks at the H* distance, there may be little or no net pressure acting on the tube for some distance above H*. In Tables 6-18 and 6-19, the fourth increment in the step that occurs two steps prior to the last step suggests that there may be no contact between the tube and tubesheet, over a portion of the circumference, for a distance above H*. Is the conclusion in 6.2.5.3 valid for the entire H* distance, given the possibility that the tubes may contain through-wall cracks at that location.* |

| | | |
|---|---|---|
| | *CPSES* | *4. Reference 1, page 6-70: In Section 6.2.5.3, it is concluded that the tube outside diameter and the tubesheet tube bore inside diameter always maintain contact in the predicted range of tubesheet displacements. However, for tubes with through-wall cracks at the H* distance, there may be little or no net pressure acting on the tube for some distance above H*. In Tables 6-18 and 6-19, the fourth increment in the step that occurs two steps prior to the last step suggests that there may be no contact between the tube and tubesheet, over a portion of the circumference, for a distance above H*. Is the conclusion in Section 6.2.5.3 valid for the entire H* distance, given the possibility that the tubes may contain through-wall cracks at that location?* |
| | *Seabrook* | *4. Reference 1, Page 6-69: In Section 6.2.5.3, it is concluded that the tube outside diameter and the tubesheet tube bore inside diameter always maintain contact in the predicted range of tubesheet displacements. However, for tubes with through-wall cracks at the H* distance, there may be little or no net pressure acting on the tube for some distance above H*. In Tables 6-18 and 6-19, the fourth increment in the step that occurs two steps prior to the last step suggests that there may be no contact between the tube and tubesheet, over a portion of the circumference, for a distance above H*. Is the conclusion in 6.2.5.3 valid for the entire H* distance, given the possibility that the tubes may contain through-wall cracks at that location?* |

Reference 10 provided follow-up questions to RAI#4. In Reference 10, the follow questions to RAI#4 were titled RAI#1. The follow-up questions from Reference 10 are reproduced below:

**RAI#1 (Reference 10)**

1. *Address following questions as part of response to RAI 4 (Vogtle):*

    a. *Clarify the nature of the finite element model ("slice" model versus axisymmetric SG assembly model) used to generate the specific information in Tables 6-1, 2, and 3 (and accompanying graph entitled "Elliptical Hole Factors") of Reference 6-15. What loads were applied? How was the eccentricity produced in the model? (By modeling the eccentricity as part of the geometry? By applying an axisymmetric pressure the inside of the bore?) Explain why this model is not scalable to lower temperatures.*

    b. *Provide table showing maximum delta diameters (total diameter distortion) and maximum eccentricities (maximum diameter minus minimum diameter) from the 3 dimensional (3-D) finite element analysis for normal operating and steam line break (SLB), for model F and D5.*

    c. *In Figure 2 of the White Paper, add plot for original relationship between reductions in contact pressure and eccentricity as given in Reference 6-15 in the graph*

*accompanying Table 6-3. Explain why this original relationship remains conservative in light of the new relationship. Explain the reasons for the differences between the curves.*

d. *When establishing whether contact pressure increases when going from normal operating to steam line break conditions, how can a valid and conservative comparison be made if the normal operating case is based on the original delta contact pressure versus eccentricity curve and the SLB case is based on the new curve?*

Response:

The responses to RAI#4 of References 5, 6 and 7 and to the follow-up question, RAI#1 of Reference 10, will be provided under separate cover.

| | | |
|---|---|---|
| ***RAI*** | *Vogtle* | *5. Reference 1, Page 6-87: -Are the previously calculated scale factors and delta D factors in Section 6.3 conservative for steam line break and feedwater line break? Are they conservative for an intact divider plate assumption? Are they conservative for all values of primary pressure minus crevice pressure that may exist along the H* distance for intact tubes and tubes with through-wall cracks at the H* distance? How is tube temperature (TT) on page 6-87 determined? For normal operating conditions, how is the TT assumed to vary as function of elevation?* |
| | *WCGS* | *5. Reference 1, Section 6.3: Please verify if the previously calculated scale factors and delta D factors in Section 6.3 conservative for (1) steam line break (SLB) and a feedwater line break (FLB); (2) an intact divider plate assumption; and (3) all values of primary pressure minus crevice pressure that may exist along the H* distance for intact tubes and tubes with through-wall cracks at the H* distance.* |
| | *B/B* | *5. Reference 1, Page 6-86, Section 6: Are the previously calculated scale factors and delta D factors in Section 6.3 conservative for steam line break and feedwater line break (FLB)? Are they conservative for an intact divider plate assumption? Are they conservative for all values of primary pressure minus crevice pressure that may exist along the H* distance for intact tubes and tubes with through-wall cracks at the H* distance?* |
| | *CPSES* | *5. Reference 1, Section 6.3, Page 6-86: Please verify if the previously calculated scale factors and delta D factors in Section 6.3 are conservative for (1) a steam line break (SLB) and a feedwater line break (FLB); (2) an intact divider plate assumption; and (3) all values of primary pressure minus crevice pressure that may exist along the H* distance for intact tubes and tubes with through-wall cracks at the H* distance.* |
| | *Seabrook* | *5. Reference 1, Section 6.3: Are the previously calculated scale factors and delta D factors in Section 6.3 conservative for steam line break (SLB) and feed line break (FLB)? Are they conservative for an intact divider plate assumption? Are they conservative for all values of primary pressure minus crevice pressure that may exist along the H* distance for intact tubes and tubes with through-wall cracks at the H* distance?* |

Response:

*Note: The page reference, 6-87 (Model F) appear to be incorrect in the question. Section 6.3 begins on page 6-83 (Model F). The page reference for the Model D5 is correct as stated in the Byron/Braidwood RAI.*

1) The previously calculated scale factors and delta D factors in Section 6.3 are conservative for all of the analyzed Model F and Model D5 conditions, including normal operating, steam line break and feedwater line break, as appropriate. Use of the contact pressure data described in Reference RAI5-1 would increase the tube-to-tubesheet contact pressure in the Model F H* analysis.

2) The previously calculated scale factors and delta D factors in Section 6.3 are conservative for an intact divider plate assumption. The results on page 6-87 assume that a greater level of weld and divider plate degradation exists in the SG (DPF = [ ]$^{a,c,e}$) than in the rest of the H* structural analysis (DPF = [ ]$^{a,c,e}$). (DPF = Divider Plate Factor).

3) The previously calculated scale factors and delta D factors in Section 6.3 are conservative for all values of primary pressure minus crevice pressure regardless of their location within the tubesheet. This is because the calculated scale factors and delta D factors applied unit pressure loads to either side of the tube and weld structure in the model such that either the primary side of the tube and tubesheet were pressurized or the secondary side of the tube and tubesheet (including the crevice) were pressurized. In the reference elliptical hole study, the gap elements that were selected for use in the two dimensional study also penalized the tube-tubesheet contact pressure by preventing line on line contact between the tube outside diameter (OD) and the tubesheet/sleeve inside diameter (ID) which results in a lower estimate of the tube-to-tubesheet contact pressure.

4) The tube temperature ($T_T$) is assumed to be equal to the primary fluid temperature for the operating condition of interest. The tube temperature is assumed to not vary as a function of elevation within the tubesheet.

<u>RAI5 References</u>:

RAI5-1. LTR-NRC-09-26, "LTR-SGMP-09-66 P-Attachment, "White Paper: Low Temperature Steam Line Break Contact Pressure and Local Tube Bore Deformation Analysis for H*"(Proprietary)," May 13, 2009

| | | |
|---|---|---|
| ***RAI*** | *WCGS* | *6. Reference 1, page 6-87: Please provide information on how the tube temperature ($T_T$) on page 6-87 was determined? For normal operating conditions, how is the $T_T$ assumed to vary as function of elevation?* |
| | *B/B* | *6. Reference 1, Page 6-9: How is tube temperature ($T_T$) on page 6-96 determined? For normal operating conditions, how is the $T_T$ assumed to vary as a function of elevation?* |
| | *CPSES* | *6. Reference 1, page 6-96: Please provide information on how the tube temperature ($T_T$) on page 6-96 was determined. For normal operating conditions, please explain how the $T_T$ is assumed to vary as function of elevation.* |
| | *Seabrook* | *6. Reference 1, Page 6-8: How is tube temperature ($T_T$) on page 6-87 determined? For normal operating conditions, how is the $T_T$ assumed to vary as function of elevation?* |

Response:

The tube temperature ($T_T$) is assumed to be equal to the primary fluid temperature for the operating condition of interest. The tube temperature is assumed to not vary as a function of elevation within the tubesheet.

| | | |
|---|---|---|
| ***RAI*** | *Vogtle* | *6. Reference 1, page 6-97, Figure 6-75:-Contact pressures for nuclear plants with Model F SGs are plotted in Figure 6-75, but it is not clear what operating conditions are represented in the plotted data, please clarify.* |
| | *WCGS* | *7. Reference 1, page 6-97, Figure 6-75: Contact pressures for nuclear plants with Model F SGs are plotted in Figure 6-75, but it is not clear what operating conditions are represented in the plotted data. Please clarify.* |
| | *B/B* | *7. Reference 1, Page 6-104, Figure 6-77: Contact pressures for nuclear plants with Model D5 steam generators are plotted in Figure 6-77, but it is not clear what operating conditions are represented for the plants shown in the plotted data; please clarify.* |
| | *CPSES* | *7. Reference 1, page 6-104, Figure 6-77: Contact pressures for nuclear plants with Model D5 SGs are plotted in Figure 6-77, but it is not clear what operating conditions are represented for the plants shown in the plotted data. Please clarify.* |
| | *Seabrook* | *7. Reference 1, Page 6-97, Figure 6-75: Contact pressures for nuclear plants with Model F steam generators are plotted in Figure 6-75, but it is not clear what operating conditions are represented in the plotted data, please clarify.* |

Response:

Figure 6-75 (WCAP-17071-P) shows the contact pressure results for the fleet of Model F steam generators for the main feedwater line break (FLB), main steam line break (SLB) and normal operating low average temperature (NOP Low $T_{avg}$) conditions. Figure RAI6-1 provides an update of Figure 6-75 in WCAP-17071-P with an expanded legend that describes each curve in the figure.

Figure 6-77 (WCAP-17072-P) shows the contact pressure results for the fleet of Model D5 steam generators for the main feed line break (FLB), main steam line break (SLB) and normal operating low average temperature (NOP Low $T_{avg}$) conditions. Figure RAI6-2 provides an update of Figure 6-77 in WCAP-17072-P with an expanded legend that describes each curve in the figure.

**Figure RAI-6-1**
**Revised Figure 6-75 (WCAP-17071-P)**

a,c,e

**Figure RAI6-2**
**Revised Figure 6-77 (WCAP-17072-P)**

a,c,e

| | | |
|---|---|---|
| **RAI** | *Vogtle* | *7. Reference 1, page 6-113, Reference 6-5: This reference seems to be incomplete; please provide a complete reference.* |
| | *WCGS* | *8. Reference 1, page 6-112, Reference 6-5: This reference seems to be incomplete. Please provide a complete reference.* |
| | *B/B* | *8. Reference 1, Page 6-120, Reference 6-5: This reference seems to be incomplete; please provide a complete reference.* |
| | *CPSES* | *8. Reference 1, page 6-120, Reference 6-5: This reference appears to be incomplete. Please provide a complete reference.* |
| | *Seabrook* | *8. Reference 1, Page 6-112, Reference 6-5: This reference seems to be incomplete; please provide a complete reference.* |

Response:

The complete reference is:

Slot, Thomas, "Stress Analysis of Thick Perforated Plates," TECHNOMIC Publishing Company, Inc., Westport, Connecticut, 1972.

| | | |
|---|---|---|
| ***RAI*** | *Vogtle* | *8. Reference 1, page 6-113, Reference 6-15: Table 6-3 in Reference 6-15 (SM-94-58, Rev 1) appears inconsistent with Table 6-2 in the same reference. Explain how the analysis progresses from Table 6-2 to Table 6-3.* |
| | *WCGS* | *9. Reference 1, page 6-113, Reference 6-15: Table 6-3 in Reference 6-15 (SM-94-58, Revision 1) appears inconsistent with Table 6-2 in the same reference. Please explain how the analysis progresses from Table 6-2 to Table 6-3.* |
| | *B/B* | *9. Reference 1, Page 6-121, Reference 6-15: Table 6-3 in Reference 6-15 (SM-94-58, Rev. 1) appears inconsistent with Table 6-2 in the same reference. Explain how the analysis progresses from Table 6-2 to Table 6-3.* |
| | *CPSES* | *9. Reference 1, Page 6-121, Reference 6-15: Table 6-3 in Reference 6-15 (SM-94-58, Revision 1) appears to be inconsistent with Table 6-2 in the same reference. Please explain how the analysis progresses from Table 6-2 to Table 6-3.* |
| | *Seabrook* | *9. Reference 1, Page 6-113, Reference 6-15: Table 6-3 in Reference 6-15 (SM-94-58, Rev 1) appears inconsistent with Table 6-2 in the same reference. Explain how the analysis progresses from Table 6-2 to Table 6-3* |

Response:

The values for initial and final eccentricity for the contact pressure ratio of 0.91 listed in Table 6-3 of Reference 6-15 (SM-94-58, Rev. 1) are calculated as follows using the values from Table 6-2:

Initial Eccentricity = (Dmax-Dmin)/ [ ]$^{a,c,e}$ inch Tube Hole ID = [ ]$^{a,c,e}$

Final Eccentricity = ((Hole Delta D (90°) – Hole Delta D (0°))/ [ ]$^{a,c,e}$ inch Tube Hole ID) =[ ]$^{a,c,e}$

The values for eccentricity in Table 6-2 of the reference should have been divided by the nominal diameter of the tubesheet hole [ ]$^{a,c,e}$ inch) to be consistent with Table 6-3.

| | | |
|---|---|---|
| ***RAI*** | *Vogtle* | *9. Reference 1, page 8-9, Figure 8: -There is an apparent discontinuity in the plotted data of the adjustment to H* for distributed crevice pressure, please provide any insight you may have as to why this apparent discontinuity exists.* |
| | *WCGS* | *10. Reference 1, page 8-9, Figure 8-1: There is an apparent discontinuity in the plotted data of the adjustment to H* for distributed crevice pressure. Please provide any insight you may have as to why this apparent discontinuity exists.* |
| | *B/B* | *10. Reference 1, page 8-9, Figure 8-1: There is an apparent discontinuity in the plotted data of the adjustment to H* for distributed crevice pressure. Please provide any insight you may have as to why this apparent discontinuity exists.* |
| | *CPSES* | *10. Reference 1, page 8-9, Figure 8-1: There is an apparent discontinuity in the plotted data of the adjustment to H* for distributed crevice pressure. Please provide any insight you may have as to why this apparent discontinuity exists.* |
| | *Seabrook* | *10. Reference 1, Page 8-9, Figure 8-1: There is an apparent discontinuity in the plotted data of the adjustment to H* for distributed crevice pressure, please provide any insight you may have as to why this apparent discontinuity exists.* |

Response:

Figure 8-1 (WCAP-17071-P, WCAP-17072-P) summarizes the variability cases run to determine the H* value response to variation of the input parameters ($\alpha_T$, $\alpha_{TS}$, $E_T$, $E_{TS}$) individually or in combination. The values of the variables were chosen to provide sufficient data to define the potential surface of interactions between the variables. No attempt was made to bias the variables in a manner that would yield H* values in the range between 3.8 inches and 4.2 inches; therefore this gap is coincidental.

Figure RAI9-1 shows a composite of the $P_{crev}$ corrections for all of the models of SGs considered, Models F, D5, 44F and 51F SGs under H* (Ref: WCAP-17071-P, WCAP-17072-P, WCAP-17091-P and WCAP-17092-P). Figure RAI9-1 shows the same characteristic shape of the $P_{crev}$ correction but also shows that the H* responses are different for the different structures. The "apparent discontinuity" in the curve for the Model F is much less pronounced for the Model D5 and other models of SG and, in the case of the Model 44F, is populated by calculated data points. Because the same analysis methods are employed for all of the Model-specific structures, it is concluded that the apparent discontinuity in Figure 8-1 of WCAP-17071-P and WCAP-17072-P is related principally to the structural response of the specific SG model being addressed, and does not imply a potential calculation error.

Figure RAI9-1 also shows that in each of the structures considered, there are steps in the $P_{crev}$ correction curves (e.g., between 3.8 and 4.2 inches in the Model F, at about 6.6 inches in the Model D5, at about 3.5 inches and 4.5 inches for the Model 44F and 51F). To investigate the step in the curve between initial predictions of H* and the $P_{crev}$ correction, several cases were considered for the Model F SGs for H* values between 3.8 inches and 4.2 inches as a typical case to evaluate the issue generically. These cases were synthesized by adjusting the values of the four influencing parameters ($\alpha_T$, $\alpha_{TS}$, $E_T$ and $E_{TS}$), based on interpolation among existing variabilities, in an attempt to yield H* values in this range. Each of the four parameters was adjusted in at least one case to meet this objective.

The following are the additional cases that were examined:

| Input Parameters | | | | H*(raw) | $P_{crev}$ | Comment |
|---|---|---|---|---|---|---|
| $a_{TS}$ | $E_{TS}$ | $a_T$ | ET | | | |
| 1 | -1 | -2 | -2 | | | Original Case |
| 5 | 4 | 0 | 0 | | | |
| -1 | 0 | -3.25 | 0 | | | |
| -1 | 0 | -3 | -5 | | | |
| 4.5 | 0 | 0 | 0 | | | |
| 5 | 4 | 0 | -1 | | | |
| 4.5 | 0 | 0 | -1 | | | |
| 5 | 0 | 0 | 0 | | | Original Case |

[ ]a,c,e

Figure RAI9-2 shows the results of this study. The $P_{crev}$ correction values are essentially constant within the narrow range of initial H* predictions that define the step in the overall curve, Figure RAI9-1, except for a single point at approximately [ ]a,c,e inches. As discussed below, the interpolation between the limited number of points representing the crevice pressure distribution and the fixed number of points representing the thickness of the tubesheet leads to isolated conditions at which the integration scheme cannot converge to a single value. A minor departure (less than about 0.005 inch) in either direction results in convergence of the integration. The point at [ ]a,c,e inches is at such a condition. It does not suggest that the crevice pressure correction is undefined at that location.

As described in each of the H* WCAP reports, the correction for $P_{crev}$ is an iterative process. Following the initial prediction of H*, which assumes that a tube separation is located at the primary face of the tubesheet and, therefore, assumes the crevice pressure is distributed over the entire thickness of the tubesheet, the calculation process depicted in Figure 1-1 of the report is repeated but with the crevice pressure distributed over the length of the initial prediction of H*. The resulting prediction of H* will exceed the initial prediction. This process is iterated until the input values and output values of H* converge to the same number. The convergence criteria are set to 2 decimals because the H* distance cannot practically be measured to the second decimal. In some instances, depending on the specific combination of input parameters that lead to the initial prediction of H*, the variation of H* is less than the convergence criteria. In that case, the default is at the larger value of the $P_{crev}$.

The H* integrator model utilizes discrete, dimensionally fixed points through the thickness of the tubesheet to represent the tube to tubesheet contact pressure. The representation of the distributed crevice pressure as discussed in Section 6 of the report utilizes a discrete number of points whose axial dimensions vary according to the assumed position of the flaw. Thus, the same number of points describes the crevice pressure profile regardless if the flaw is assumed at the bottom of the tubesheet or at some other location within the tubesheet. Only the slope of the distribution between the points changes. Because of a mismatch between the crevice pressure axial definition and the tubesheet contact pressure axial definition, the integration model cannot converge to a single value at certain discrete points, depending on the model of SG under consideration. For the Model F SG, this point occurs at approximately 4 inches from the top of the tubesheet. The axial range within which this occurs is extremely narrow, less than [ ]$^{a,c,e}$ inch (see Figure RAI9-2), and the non-convergence results in a very limited range of the axial crevice pressure correction factor, less than [ ]$^{a,c,e}$ inch. For the Model F SG, a variation of initial H* prediction of approximately 0.005 inch from the critical axial length results in the model converging again at the lower value of $P_{crev}$ correction as also shown on Figure RAI9-2. This result applies generically to the Model D5, 44F and 51F SGs as well.

For practical application in determining the final value of H*, it is noted that when the adjustments for BET and NOP thermal distribution are included, the predicted values of H* are far removed from the points in the $P_{crev}$ correction curves where the model does not converge for all models of SGs. The recommended values of H*, prior to the correction for $P_{crev}$, for the different models of SG are:

| | |
|---|---|
| Model F: | 9.81 inches (Ref: WCAP-17071-P) |
| Model D5 | 12.11 inches (Ref: WCAP-17072-P) |
| Model 44F | 11.06 inches (Ref: WCAP-17091-P) |
| Model 51F | 11.14 inches (Ref: WCAP-17092-P) |

In all cases, the point of non-convergence of the model does not affect the final recommended value of H*.

**Figure RAI9-1**
**$P_{crev}$ Correction Profiles for Models F, D5, 44F and 51F SGs**

[ ] a,c,e

**Figure RAI9-2**

a,c,e

[ ]

| | | |
|---|---|---|
| ***RAI*** | *Vogtle* | *10. Reference 1, Page 8-6, Section 8.1.4: Clarify whether the "biased" H* distributions for each of the four input variables are sampled from both sides of the mean H* value during the Monte Carlo process, or only on the side of the mean H* value yielding an increased value of H*.* |
| | *WCGS* | *11. Reference 1, Page 8-6, Section 8.1.4: Please clarify whether the "biased" H* distributions for each of the four input variables are sampled from both sides of the mean H* value during the Monte Carlo process, or only on the side of the mean H* value yielding an increased value of H*.* |
| | *B/B* | *11. Reference 1, Page 8-6, Section 8.1.4: Clarify whether the "biased" H* distributions for each of the four input variables are sampled from both sides of the mean H* value during the Monte Carlo process, or only on the side of the mean H* value yielding an increased value of H*.* |
| | *CPSES* | *11. Reference 1,Page 8-6, Section 8.1.4: Please clarify whether the "biased" H* distributions for each of the four input variables are sampled from both sides of the mean H* value during the Monte Carlo process, or only on the side of the mean H* value yielding an increased value of H*.* |
| | *Seabrook* | *11. Reference 1, Page 8-6, Section 8.1.4: Clarify whether the "biased" H* distributions for each of the four input variables are sampled from both sides of the mean H* value during the Monte Carlo process, or only on the side of the mean H* value yielding an increased value of H** |

Response:

As shown in Figure 8-11 of the report (WCAP-17071-P, WCAP-17072-P, WCAP-17091-P and WCAP-17092-P), the variation of the parameters that resulted in the greatest increase in the value of H* were chosen as the "biased" influence factors from which to sample in the Monte Carlo (MC) process. These distributions were normal distributions determined from the mean H* and greatest H* variation resulting from equal valued positive and negative variations of the respective parameters. Note that for the case of coefficient of thermal expansion of the tube, a decrease in the coefficient results in an increase in the H* value and also reflects the broadest distribution. For the coefficient of thermal expansion of the tubesheet, an increase in the coefficient results in increasing H* and also results in the broadest distribution.

Both sides of the biased influence factors were sampled during the Monte Carlo analysis. Sampling from the broadest distributions results in the broadest H* distribution and the largest values of H* corresponding to the desired probabilistic goal, in this case, 95/50.

Figure RAI10-1 shows the results of the Monte Carlo sampling from the interaction surface (see RAI#20) for the resulting values of H* between the upper 93% and 98% of the simulations. (The 98% upper limit was chosen for convenience). The highest values

of H* are concentrated in a well defined region bounded approximately by the tube coefficient of thermal expansion ($\alpha_T$) between [ ]$^{a,c,e}$ and tubesheet coefficient of thermal expansion ($\alpha_{TS}$) between [ ]$^{a,c,e}$ The conclusion that the maximum values of H* are produced from samples in approximately the center of the interaction surface defined by Figure 8-5 in the report applies to both the Model F and Model D5 SGs. Consequently, the use of the broadest distributions that increase the value of H* will tend to focus on the region in question because the broadest H* distributions are defined by negative variations of $\alpha_T$ and by positive variations of $\alpha_{TS}$. Selections from the negative sides of the broadest distributions will not result in maximum values of H*. If picks are made from both distributions on the negative side of the biased influence distributions, the result will be an over-prediction of the lower tail of the H* distribution. This is noted in WCAP-17071-P, WCAP-17072-P, WCAP-17091-P and WCAP17092-P and is of no consequence because only the maximum value of H* is of concern.

**Figure RAI10-1**

a,c,e

***Figure RAI10-2***

a,c,e

| | | |
|---|---|---|
| ***RAI*** | *Vogtle* | *11. Reference 1, page 8-14, Figure 8-6: The legend for one of the interactions shown between $\alpha_{TS}$ and $E_{TS}$ appears to have a typo in it, please review and verify that all values shown in the legend are correct.* |
| | *WCGS* | *12. Reference 1, page 8-14, Figure 8-6: The legend for one of the interactions shown between the coefficient of thermal expansion of the tube ($\alpha_{TS}$) and tubesheet ($E_{TS}$) appears to contain typographical error. Please review and verify that all values shown in the legend are correct.* |
| | *B/B* | *12. Reference 1, Page 8-14, Figure 8-6: The legend for one of the interactions shown between $\alpha_{TS}$ and $E_{TS}$ appears to have a typo in it. Please review and verify that all values shown in the legend are correct.* |
| | *CPSES* | *12. Reference 1, page 8-14, Figure 8-6: The legend for one of the interactions shown between the coefficient of thermal expansion of the tubesheet ($\alpha$TS) and Young's modulus of the tubesheet (ETS) appears to contain a typographical error. Please review and verify that all values shown in the legend are correct.* |
| | *Seabrook* | *12. Reference 1, Page 8-14, Figure 8-6: The legend for one of the interactions shown between $\alpha_{TS}$ and $E_{TS}$ appears to have a typo in it, please review and verify that all values shown in the legend are correct.* |

Response:

The uppermost curve, defined by the star point, which is currently labeled as $a_{TS}$=-3 should be labeled as $a_{TS}$=+3. All other values in the legend are correct.

| | | |
|---|---|---|
| ***RAI*** | *Vogtle* | *12. Reference 1, page 8-20, Case S-4: Why does the assumption of a 2-sigma value for the coefficient of thermal expansion of the tube ($\alpha T$) and the tubesheet ($\alpha TS$) to determine a "very conservative biased mean value of H*" conservatively bound the interaction effects between $\alpha T$ and $\alpha TS$? Describe the specifics of how the "very conservative biased mean value of H*," as shown in Table 8-4, was determined.* |
| | *WCGS* | *13. Reference 1, page 8-20, Case S-4: Why does the assumption of a 2-sigma value for the coefficient of thermal expansion of the tube ($\alpha T$) and the tubesheet ($\alpha TS$) to determine a "very conservative biased mean value of H*" conservatively bound the interaction effects between $\alpha T$ and $\alpha TS$? Please describe the specifics of how the "very conservative biased mean value of H*," as shown in Table 8-4, was determined.* |
| | *B/B* | *13. Reference 1, Page 8-20, Case S-4: Why does the assumption of a 2-sigma value for the coefficient of thermal expansion of the tube ($\alpha_T$) and the tubesheet ($\alpha_{TS}$) to determine a "very conservative biased mean value of H*" conservatively bound the interaction effects between $\alpha_T$ and $\alpha_{TS}$? Describe the specifics of how the "very conservative biased mean value of H*," as shown in Table 8-4, was determined.* |
| | *CPSES* | *13. Reference 1, page 8-20, Case S-4: Why does the assumption of a 2-sigma value for the coefficient of thermal expansion of the tube ($\alpha T$) and tubesheet ($\alpha TS$) to determine a "very conservative biased mean value of H*" conservatively bound the interaction effects between $\alpha T$ and $\alpha TS$? Please describe how the "very conservative biased mean value of H*," as shown in Table 8-4, was determined.* |
| | *Seabrook* | *13. Reference 1, Page 8-20, Case S-4: Why does the assumption of a 2-sigma value for the coefficient of thermal expansion of the tube ($\alpha T$) and the tubesheet ($\alpha TS$) to determine a "very conservative biased mean value of H*" conservatively bound the interaction effects between $\alpha T$ and $\alpha TS$? Describe the specifics of how the "very conservative biased mean value of H*," as shown in Table 8-4, was determined.* |

Response:

The very conservative mean value of H*, [ ]$^{a,c,e}$ inches (Model F), [ ]$^{a,c,e}$ inches, (Model D5), is determined by arbitrarily assuming that the 2-sigma values of all variables defines the mean value of H*. To determine these values, it was assumed that the input variables to the structural evaluation (i.e, the entire H* calculation process as shown in

Figure 1-1 of the report) were set at their 2-sigma values, and the resulting H* was termed the "conservative mean." Table RAI12-1 illustrates the input values that define the mean value of H* and the "very conservative mean" value of H*. The SRSS approach was then applied using the influence factors from Table 8-2 in the report for the 95/50 whole-bundle value appropriate to the model SG being considered. The result is essentially equivalent to the 5-sigma variation case, Case S4 on Table 8-3 of the report. Note that because the 2-sigma input parameter value of H* was determined by the entire calculation process shown in Figure 1-1 of WCAP, the interaction effects of the variables at the 2-sigma level are included in this calculation.

**Table RAI12-1**
**Definition of "Conservative Mean" H***

| Definition | Analysis Input Parameters and their Values | | | |
|---|---|---|---|---|
| | $\alpha_T$ | $\alpha_{TS}$ | $E_T$ | $E_{TS}$ |
| Mean H* | mean | mean | mean | mean |
| Conservative Mean H* | Mean-2σ(1) | Mean+2σ(1) | Mean-2σ(1) | Mean-2σ(1) |
| (1) Values chosen in direction of increasing H* | | | | |

| | | |
|---|---|---|
| ***RAI*** | *Vogtle* | *13. Reference 1, page 8-22, Case M-5: The description for this case seems to correspond to a single tube H* estimate rather than a whole bundle H* estimate. How is the analysis performed for a whole bundle H* estimate?* |
| | *WCGS* | *14. Reference 1, page 8-22, Case M-5: The description for this case seems to correspond to a single tube H* estimate rather than a whole bundle H* estimate. Please explain how is the analysis performed for a whole bundle H* estimate?* |
| | *B/B* | *14. Reference 1, Page 8-22, Case M-5: The description for this case seems to correspond to a single tube H* estimate rather than a whole bundle H* estimate. How is the analysis performed for a whole bundle H* estimate?* |
| | *CPSES* | *14. Reference 1, page 8-22, Case M-5: The description for this case seems to correspond to a single tube H* estimate rather than a whole bundle H* estimate. Please explain how the analysis is performed for a whole bundle H* estimate?* |
| | *Seabrook* | *14. Reference 1, Page 8-22, Case M-5: The description for this case seems to correspond to a single tube H* estimate rather than a whole bundle H* estimate. How is the analysis performed a whole bundle H* estimate?* |

Response:

Case M-5 is the Monte Carlo (MC) sampling analogy to Case S-2. A single tube analysis would sample from the 1$\sigma$ influence distributions to determine the overall distribution of H*, and from the resulting H* distribution, choose the 95% probability value of the upper tail. Case M-5 pre-biases the influence factor distributions by choosing the influence factor distributions at the 4.285$\sigma$ (Model F) (4.237$\sigma$ Model D5) values divided by 4.285 (Model F) (4.237, Model D5). Thus, the input distributions are pseudo-1$\sigma$distributions that are already biased by the number of standard deviations required to represent a whole bundle analysis as was done in Case S-2. The use of the greater value influence functions results in a broader final H* distribution from which the 95/50 value represents the whole bundle. The basis for the 4.285$\sigma$ (Model F)(4.237$\sigma$, Model D5) value to represent the whole bundle case is discussed in the report.

It was recognized that the assumption of normality of the influence factor distribution could influence the results from the MC approach included in the report. Nevertheless, the MC cases were included in the report to provide a basis for evaluating multiple variability cases that could not be considered using the SRSS approach. The response to RAI#20 provides a comprehensive analysis based on the interaction surface of Figure 8-5 and utilization of the Monte Carlo technique.

| | | |
|---|---|---|
| ***RAI*** | *Vogtle* | *14. Reference 1, page 8-2: Case M-5 states, "Interaction effects are included because the 4.285 sigma variations were used that already include the effective interactions among the variables." Case M-5 also states that the 4.285 sigma variations come from Table 8-2. However, Table 8-2 does not appear to include interactions among the variables. Explain how the 4.285 sigma variations include the effect of interactions among the variables.* |
| | *WCGS* | *15. Reference 1, page 8-22: Case M-5 states, "Interaction effects are included because the 4.285 sigma variations were used that already include the effective interactions among the variables." Case M-5 also states that the 4.285 sigma variations come from Table 8-2; however, Table 8-2 does not appear to include interactions among the variables. Please explain how the 4.285 sigma variations include the effect of interactions among the variables.* |
| | *B/B* | *15. Reference 1, Page 8-22: Case M-5 states, "Interaction effects are included because the 4.237 sigma variations were used that already include the effective interactions among the variables." Case M-5 also states that the 4.237 sigma variations come from Table 8-2. However, Table 8-2 does not appear to include interactions among the variables. Explain how the 4.237 sigma variations include the effect of interactions among the variables.* |
| | *CPSES* | *15. Reference 1, page 8-22: Case M-5 states, "Interaction effects are included because the 4.237 sigma variations were used that already include the effective interactions among the variables." Case M-5 also states that the 4.237 sigma variations come from Table 8-2; however, Table 8-2 does not appear to include interactions among the variables. Please explain how the 4.237 sigma variations include the effect of interactions among the variables.* |
| | *Seabrook* | *15. Reference 1, Page 8-22: Case M-5 state,: "Interaction effects are included because the 4.285 sigma variations were used that already include the effective interactions among the variables." Case M-5 also states that the 4.285 sigma variations come from Table 8-2. However, Table 8-2 does not appear to include interactions among the variables. Explain how the 4.285 sigma variations include the effect of interactions among the variables* |

Response:

Because the 4.285σ (Model F), 4.237σ (Model D5) variations were calculated using the complete calculation process depicted in Figure 1-1 of the report (WCAP-17071-P, WCAP-17072-P), the variations include the structural interaction effects for each variable assuming that all other variables are at their mean value. If multiple variables were

perturbed simultaneously, a greater effect on H* would be expected. The Monte Carlo sampling scheme used did not support the use of compound parameter variations.

The response to RAI#20 provides an in-depth analysis of the interaction effects among the significant variables using the Monte Carlo method and sampling from the interaction surface of Figure 8-5.

| | | |
|---|---|---|
| ***RAI*** | *Vogtle* | *15. Reference 1, page 8-22, Case M-6, first bullet: Should the words "divided by 4.285" appear at the end of the sentence?* |
| | *WCGS* | *16. Reference 1, page 8-22, Case M-6, first bullet: Please verify if the words "divided by 4.285" appear at the end of the sentence.* |
| | *B/B* | *16. Reference 1, Page 8-22, Case M-6, first bullet: Should the words "divided by 4.237" appear at the end of the sentence?* |
| | *CPSES* | *16. Reference 1, page 8-22, Case M-6, first bullet: Please verify if the words "divided by 4.237" should appear at the end of the sentence?* |
| | *Seabrook* | *16. Reference 1, Page 8-22, Case M-6, first bullet: Should the words "divided by 4.285" appear at the end of the sentence?* |

Response:

The first bullet under Case M-6 on page 8-22 is clarified by adding the phrase "divided by 4.285" (Model F) ("4.237"-Model D5) between "4.285σ" (Model F) ("4.237σ"-Model D5) and "from."

| | | |
|---|---|---|
| ***RAI*** | *Vogtle* | *16. Reference 1, page 8-23, Case M-7: Was the "2 sigma variation of all variables" divided by a factor of 2?* |
| | *WCGS* | *17. Reference 1, page 8-23, Case M-7: Please verify if the "2 sigma variation of all variables" divided by a factor of 2.* |
| | *B/B* | *17. Reference 1, Page 8-23, Case M-7: Was the "2 sigma variation of all variables" divided by a factor of 2?* |
| | *CPSES* | *17. Reference 1, page 8-23, Case M-7: Please verify if the "2 sigma variation of all variables" was divided by a factor of 2.* |
| | *Seabrook* | *17. Reference 1, Page 8-23, Case M-7: Was the "2 sigma variation of all variables" divided by a factor of 2?* |

Response:

For case M-7, the 2-sigma variation was treated as if it were 1-sigma variation. This assumption is somewhat arbitrary and intended only as a hypothetical case to show the effect on H* if it were assumed that the calculated standard deviation are much larger. Therefore, the 2-sigma variation was NOT divided by 2.

This case is an arbitrary sensitivity study that addresses the H* result if the 1$\sigma$ influence factors were more than doubled. Starting from the basic mean structural prediction of H*, [ ]$^{a,c,e}$ for the Model F ([ ]$^{a,c,e}$, for the Model D5) inches, it was assumed that the 2$\sigma$ influence distributions applied instead of the 1$\sigma$ influence distributions, and the MC sampling was from the 2$\sigma$ distributions. The principal objective of this case was to show that very conservative assumptions do not lead to a major impact on the value of H*.

| | | |
|---|---|---|
| **RAI** | *Vogtle* | *17. Reference 1, page 8-23, Case M-7: Explain how this case includes the interaction effects between the two principle variables, $\alpha T$ and $\alpha TS$.* |
| | *WCGS* | *18. Reference 1, page 8-23, Case M-7: Please explain how this case includes the interaction effects between the two principle variables, $\alpha T$ and $\alpha TS$.* |
| | *B/B* | *18. Reference 1, Page 8-23, Case M-7: Explain how this case includes the interaction effects between the two principle variables, $\alpha_T$ and $\alpha_{TS}$.* |
| | *CPSES* | *18. Reference 1, page 8-23, Case M-7: Please explain how this case includes the interaction effects between the two principal variables, $\alpha T$ and $\alpha TS$.* |
| | *Seabrook* | *18. Reference 1, Page 8-23, Case M-7: Explain how this case includes the interaction effects between the two principle variables, $\alpha T$ and $\alpha TS$.* |

Response:

Case M-7 assumes that the $1\sigma$ variability of H* in the parameters is based on the $2\sigma$ influence factors calculated for each parameters. Because the influence factors are calculated using the entire calculation flow depicted in Figure 1-1 of the report, the interactive effect of the key parameters at the $2\sigma$ is reflected. The calculations were performed by perturbing one parameter at a time; therefore, the combined interaction of perturbing multiple parameters is not reflected. However, the assumption that the $2\sigma$ variation in the direction of increasing H* represent one standard deviation of the H* influence factors and the extreme value calculation process provide a very conservative estimate of H*.

The response to RAI#20 provides an in-depth analysis of the interaction effects among the significant variables.

| | | |
|---|---|---|
| **RAI** | *Vogtle* | *18. Reference 1, page 8-25, Table 8-4: Explain why the mean H* calculated in the fifth case does not require the same adjustments, as noted by the footnotes, that all other cases in the table require.* |
| | *WCGS* | *19. Reference 1, page 8-25, Table 8-4: Please explain why the mean H* calculated in the fifth case does not require the same adjustments, as noted by the footnotes, that all other cases in the table require.* |
| | *B/B* | *19. Reference 1, Page 8-25, Table 8-4: Explain why the mean H* calculated in the fifth case does not require the same adjustments, as noted by the footnotes, that all other cases in the table require.* |
| | *CPSES* | *19. Reference 1, page 8-25. Table 8-4: Please explain why the mean H* calculated in the fifth case does not require the same adjustments, as noted by the footnotes, that all other cases in the table require.* |
| | *Seabrook* | *19. Reference 1, Page 8-25, Table 8-4: Explain why the mean H* calculated in the fifth case does not require the same adjustments, as noted by the footnotes, that all other cases in the table require.* |

Response:

The superscripts referring to the notes were inadvertently omitted from the mean H* value for Case S-4 in Table 8-4. The mean value of H* shown, [ ]$^{a,c,e}$ inches (Model F) ([ ]$^{a,c,e}$ inches, Model D5), includes the adjustment for BET and for the NOP thermal distribution.

This omission exists also in WCAP-17072-P for the Model D5 SGs, but has been corrected on subsequent H* reports for the Model 44F and 51F SGs (WCAP-17091-P and WCAP17092-P).

| | | |
|---|---|---|
| ***RAI*** | *Vogtle* | *19. Reference 1, page 8-25, Table 8-4: Verify the mean H* shown in the last case in the table.* |
| | *WCGS* | *20. Reference 1, page 8-25, Table 8-4: Please verify the mean H* shown in the last case in the table.* |
| | *B/B* | *20. Reference 1, Page 8-25, Table 8-4: Verify the mean H* shown in the last case in the table.* |
| | *CPSES* | *20. Reference 1, page 8-25, Table 8-4: Please verify the mean H* shown in the last case in the table.* |
| | *Seabrook* | *20. Reference 1, Page 8-25, Table 8-4: Verify the mean H* shown in the last case in the table* |

Response:

(Please also see the response to Question 16.)

The mean value of H* for Case M7 is correct as shown on Table 8-4.

The purpose of this case was to determine the whole bundle, extreme value of H* and to show the effect on H* if the uncertainties were doubled at the same time as discussed in the response to Question 16. The process to achieve this was to calculate the mean H* as for all other cases, except case S4, on Table 8-4, but then to arbitrarily assume that the $2\sigma$ variations as the values for the $1\sigma$ influence distributions of H*. The intent of this case was to show that extreme assumptions of variability do not invalidate the H* concept.

| | | |
|---|---|---|
| ***RAI*** | *Vogtle* | *20. Section 8 of Reference 1: The variability of H* with all relevant parameters is shown in Figure 8-3. The interaction between $\alpha_T$ and $\alpha_{TS}$ are shown in Figure 8-5. Please explain why the direct relationships shown in these two figures were not sampled directly in the Monte Carlo analysis, instead of the sampling method that was chosen. Also, please explain why the sampling method chosen led to a more conservative analysis than directly sampling the relationships in Figures 8-3 and 8-5.* |
| | *WCGS* | *21. Section 8 of Reference 1: The variability of H* with all relevant parameters is shown in Figure 8-3. The interaction between $\alpha_T$ and $\alpha_{TS}$ are shown in Figure 8-5. Please explain why the direct relationships shown in these two figures were not sampled directly in the Monte Carlo analysis, instead of the sampling method that was chosen. Also, please explain why the sampling method chosen led to a more conservative analysis than directly sampling the relationships in Figures 8-3 and 8-5.* |
| | *B/B* | *21. Section 8 of Reference 1: The variability of H* with all relevant parameters is shown in Figure 8-3. The interaction between $\alpha_T$ and $\alpha_{TS}$ are shown in Figure 8-5. Please explain why the direct relationships shown in these two figures were not sampled directly in the Monte Carlo analysis, instead of the sampling method that was chosen. Also, please explain why the sampling method chosen led to a more conservative analysis than directly sampling the relationships in Figures 8-3 and 8-5.* |
| | *CPSES* | *21. Section 8 of Reference 1: The variability of H* with all relevant parameters is shown in Figure 8-3. The interaction between $\alpha_T$ and $\alpha_{TS}$ are shown in Figure 8-5. Please explain why the direct relationships shown in these two figures were not sampled directly in the Monte Carlo analysis, instead of the sampling method that was chosen. Also, please explain why the sampling method chosen led to a more conservative analysis than directly sampling the relationships in Figures 8-3 and 8-5.* |
| | *Seabrook* | *21. Section 8 of Reference 1: The variability of H* with all relevant parameters is shown in Figure 8-3. The interaction between $\alpha_T$ and $\alpha_{TS}$ are shown in Figure 8-5. Please explain why the direct relationships shown in these two figures were not sampled directly in the Monte Carlo analysis, instead of the sampling method that was chosen. Also, please explain why the sampling method chosen led to a more conservative analysis than directly sampling the relationships in Figures 8-3 and 8-5.* |

Response:

General

The recommended value of H* is based on the square root of the sum of the squares (SRSS) approach to combining the uncertainties for H*. The Monte Carlo cases included in the report were included as a vehicle to study different sensitivities to H* parameters variations and were provided as support for the SRSS recommendation. The peer review (Expert Panel's) conclusions were that the SRSS approach was a suitably conservative approach given the many conservatisms built into the H* analysis. The significant conservatisms included in the H* analysis are summarized in Section 1 of the report(s) and again identified in Section 10 of the report(s).

Figures 8-3 and 8-5 were developed during, and immediately after, the peer review of the H* project, which was followed in close order by publishing the report. The staff's observation that Figures 8-3 and 8-5 reasonably define an interaction surface, which could be utilized directly for a Monte Carlo sampling assessment, is correct. Therefore, a Monte Carlo analysis based on the interaction surface defined by Figure 8-4 in the respective WCAP reports for the different models of SGs was completed. This analysis provided the opportunity to quantify some of the conservatisms that are included in the technical justification of H*. The approach to this issue was to consider the most significant conservatisms in the overall H* analysis and quantify their effects on the recommended value of H* to show that the recommended value of H* is conservative. The sequence of the analysis was as follows:

1. Application of the Monte Carlo methodology discussed in the H* reports, except for case M-6, assumes that each simulation of H* includes a different value of the properties of the tubesheet. Thus, if 100,000 simulations are performed, each simulation includes a different random pick of tubesheet properties. Among the population of H* candidate plants, there are 60 steam generators; therefore, the actual population of tubesheets is limited to 60. To better address the limited population of tubesheets, the reference MC sampling is a staged process corresponding to the simulation of one steam generator tubesheet/tube bundle combination. A set of tubesheet properties is selected, and for that set, the corresponding tube properties are sampled 5626 times for the Model F SG tube population (4570 times for the model D5 SG tube population), and as appropriate for the other models of SGs. The above process is repeated 10,000 times. This provides a more accurate simulation reflecting the limited number of tubesheets in the population.

2. The probabilistic analysis in Section 8 of the report(s) assumes that the entire tube bundle consists of tubes located at the worst case location in the tube bundle (e.g., the most limiting radius in the most limiting sector of the tube bundle as shown in Section 6.2.3). As shown in Figure 6-1 of the report, the worst tube is defined by a very narrow segment of tubes, while all other tubes are shown to have a lower value

of H*. Therefore, the bundle was divided into a number of sectors as discussed below, and the 0.95 probability at 50% confidence value of H* was defined on the combined probability of the sector probability for all tubes. This analysis is still quite conservative because all tubes are still assumed to be in the limiting azimuthal sector of the tube bundle (the sector perpendicular to the divider plate including about 5° from the centerline of the tubesheet. See Section 6.2.3 of the report). Tubes more than about 5 pitches removed from the centerline perpendicular to the divider plate have been shown to have lower values of H*.

3. The current analysis for the Model F and Model D5 SGs includes a correction factor for the NOP thermal distribution through the tubesheet. The factor was developed very conservatively using a ratio technique (see report Section 6.2.2.2.5). This correction factor was re-evaluated (see the response to RAI#2) and a more realistic value of it is applied in this analysis. The correction factor does not apply equally to all models of SG; therefore, the effect of the correction factor is SG model-specific and has already been included in the reports for the Model 44F and Model 51F SGs (WCAP-17091-P and WCAP-17092-P). The analysis results below identify the SG models where this improved analysis applies.

4. The H* analysis assumes no contribution from residual contact pressure (RCP). All test data to date, including data from tests performed prior to 2008, has shown that a positive value of RCP exists after hydraulic expansion of the tubes. Tests were performed during the current H* program that confirmed a significant level of RCP, and also showed that within a short distance of motion, the forces required to continue to move the tube by far exceeded the maximum pull out forces that could be generated under very conservative assumptions. The analysis quantifies the effect of RCP on the calculated value of H* and benchmarks the RCP to the tests that were performed during the H* development.

A. Sector Analysis

Based on the profile of the predicted mean H*, the tube bundle is divided into 9 annular sectors as shown in Figures RAI20-1, -2, -3 and -4 for the models of SG included in the H* population (Reference RAI20-1). (In Figure RAI20-4, for the Model 51F SGs, the appropriate sector division results in only 7 sectors; however, additional sectors with 1 tube, each, were added at both ends for convenience of the calculations.) The normalized H* is determined from the raw H* calculation results, prior to adjustment of the H* value by the addition of correction factors for the BET and NOP tubesheet thermal profile. This is done to obtain a true normalization, unaffected by any constants. However, the final value of H*, after the MC sampling for ΔH, is based on the adjusted maximum mean value of H* as shown in the appropriate sector in Tables 1, 2, 3 and 4. The adjustment for crevice pressure referenced to the predicted H* is made after the all other factors have been accounted for. Thus, for each sector:

[ ] a,c,e

Where,

F is the sector normalization factor from Figures RAI20-1, -2, -3 and -4,

$H^*_{(BET+ Tnop)}$ is the raw H* value adjusted for BET and NOP thermal distribution

$\Delta H^*_{uncert}$ is the adjustment for interaction effects from the MC analysis

$\Delta H_{pcrev}$ is the adjustment for crevice pressure

The normalized value of H* in each sector is based on the maximum value of H* in that sector; thus, the sector evaluation is inherently conservative.

The number of tubes in each sector is determined from the row and column numbers and the model-specific pitch of the tubes. Tables RAI20-1, -2, -3, and -4 summarize the sector populations for each of the models of SGs.

B. Interaction Surface and Monte Carlo Sampling

A simulation model was developed to evaluate limiting values of H* for specific classes of steam generators. The Monte-Carlo based model evaluates extreme values of H* on a single steam generator basis, repeating the process to construct a distribution of maximum H* values. The final output of the model is the 95/50 estimate of extreme H* within any one steam generator.

The components of variance included in the model are the coefficients of thermal expansion (CTE's) for the tubesheet and the individual tubes. These have been shown in the H* reports to be, by far, the most significant contributors to variations in H* for the tubesheet/tube bundle combinations. The essential function describing H* variation for specific value pairs of the thermal expansion coefficients has been developed and is shown in Figure 8.5 of the H* reports. It should be noted that full interaction effects are included.

The basic structure of the simulation is shown in Figure RAI20-5 and represents one Monte Carlo trial. The process shown produces one realization of the extreme H* for a given steam generator. Repetition, involving 10,000 trials produces a distribution from which a 95/50 estimate of H*can be obtained by robust nonparametric means. As shown in Figure RAI20-5, the core process involves a random selection of one value of tubesheet CTE and N values of tube CTE, where N is the number of tubes in the steam generator or specific region of interest. The resulting N pairs are propagated through the

fitted surface to produce N values of H* which are then sorted to identify the maximum (extreme) value of H* which is stored for further use.

The above process can be easily applied on a regional (SG sector) basis by running the simulation for each region separately based on region-specific values on tube population size and average H*. The composite H* for the entire steam generator can be obtained by the following equation:

$$H^*_c = [ \qquad ]^{a,c,e} \text{ for M Region model}$$

It is most important that the H* values for the individual regions are not sorted prior to application of the above post-processing because of the need to maintain tubesheet identity between regions.

C. Sector Application of Interaction Effects

The interaction data shown in Figure 8-5 of the H* WCAPs were developed for the limiting tube radius (i.e., the tubesheet radius in Figures 1, 2, 3 and 4) where the normalized value of H* is 1. Because of the complex nature of the H* analysis, it was necessary to determine if the interaction effects at the limiting H* radius adequately represented the interactions at other tubesheet radii. Two radii were selected to represent the most probable locations where significant effects, if they exist, might materialize: 1) A tubesheet sector near the limiting radius, and 2) A tubesheet sector far removed from the limiting radius.

It was shown in the reports that the influence of Young's modulus on the final values of H* is negligible and that there was no significant interaction between the Young's moduli of the materials and the coefficient of thermal expansion of the materials. The existing interactions are limited to the coefficients of thermal expansion of the tube and tubesheet materials. Therefore, the same matrix of sensitivity cases that defined Figure 8-5 in the reports was run for each of the two tubesheet sector chosen as noted above.

In all cases it was determined that the interaction effects defined in Figure 8-5 of the report(s) for the location of the maximum mean H* value bounded the interaction effects of the other sectors considered. Therefore, for conservatism and simplicity, the range of interaction effects (i.e., $\Delta H^* = f(\alpha_T, \alpha_{TS})$) for the maximum mean value of H* shown on Figure 8-5 was applied for all sectors of the tubesheet.

Figures RAI20-6 and RAI20-7 show the results of this evaluation for the tubesheet sectors selected for the Model F and Model D5 SGs. The interaction profile for the mean, $3\sigma$ and $5\sigma$ variation of tubesheet coefficient of thermal expansion are shown to cover the significant range of variability. In all cases, the variability of the location of the maximum value of H* is greater than, or equal to, the variability at other radial locations on the tubesheet. Therefore, the application of the variability for the radial location of the maximum value of H* for all other radial locations is justified and conservative.

D. Results from Sector Based Sampling from the Interaction Surfaces

Table RAI20-5 (a) summarizes the recommended values of H* from the H* reports for all of the affected Model SGs together with the results of the Monte Carlo (MC) sampling from the interaction surface defined in Figure 8-5 of each report. The MC sampling was based on the sector approach described above and also the approach shown in Figure RAI20-5 to limit the number of tubesheet simulation. The result from this sampling must be adjusted for the crevice pressure distribution referenced to the location of the initially predicted value of H*. The correction for crevice pressure is taken from Figure 8-1 of the respective reports. After the adjustments are made for the crevice pressure reference location, the values of H* are slightly greater than the recommended values of H* from the respective reports.

Table RAI20-5(b) extends the evaluation of the conservatism of the recommended SRSS-based values of H* by adjusting the Monte Carlo sampling results for the updated values of the adder for the NOP thermal distribution in the tubesheet for the Model F and Model D5 SGs. The updated NOP thermal distribution factor for the Model 44F and Model 51F SGs are already included in the respective reports (WCAP-17091-P and WCAP-17092-P); consequently there is no adjustment made for these models of SG.

The original NOP thermal distribution adjustment factor was developed on a very conservative basis, using the scaling method described in Section 6.2.2.2.5 of WCAP-17071-P and WCAP-17072-P. As the analysis for H* evolved, a direct method of applying the tubesheet NOP thermal distribution in the structural analysis was developed; this method is describe in Section 6.2.2.2.5 of WCAP-17072-P (Model D5 report). For the Model D5 SG, the necessary correction based on the updated method was [ ]$^{a,c,e}$ inch compared to [ ]$^{a,c,e}$ inch based on the scaling technique. A similar analysis was subsequently performed for the Model F SG and it was determined that the appropriate correction for the NOP thermal distribution is [ ]$^{a,c,e}$ inch instead of the [ ]$^{a,c,e}$ inches included in the recommended value of H* in WCAP-17071-P.

When the updated correction for the NOP thermal distributions are applied, and the necessary correction for crevice pressure reference location is applied, the final value of H* for the Model F SG is [ ]$^{a,c,e}$ inches and, for the Model D5, is [ ]$^{a,c,e}$ inches (see Table RAI20-5(b)). Both of these values are less than the recommended values of H*, respectively, for the Model F and Model D5 SGs. Thus, it is concluded that the recommended values of H*, based on the SRSS approach as shown in the respective reports for the Model F and Model D5 SGs, are conservative.

It should be noted that the adjustment of the NOP thermal distribution correction factor does not impact which operating condition, NOP or SLB, is the limiting condition. The limiting value of H* is determined by three times normal operating pressure before and after the adjustment for the NOP thermal distribution. Section 6.4.5 of the Model F report, WCAP-17071-P, and the Model D5 report, WCAP-17072-P, discusses the determination of the H* values. When the NOP thermal distribution is directly included in

the structural analysis to determine tubesheet displacements, the NOP condition remains the limiting condition for H*.

E. Determination of Residual Contact Loads from Pull Out Tests

In prior analyses for H*, pull out test data has been used to calculate a residual contact pressure, which is distributed over the length of the tubesheet and included in the integration of pull out force over length to determine the length at which the pull out and resisting forces are equal. However, the pull out resistance can also be used to offset the pull out forces. Both methods were studied and it was determined that the same result was achieved, regardless of which method was applied. Because offsetting the applied loads requires fewer assumption (i.e., coefficient of friction) and results in more conservative values of H*, this approach was selected to determine the effect of the hydraulic expansion only on the calculated value of H*.

Reference RAI20-2, provided as Appendix A to this document, summarizes the pull out test program performed in support of the H* development. The data from the pull out tests and Monte Carlo simulation were used to determine a conservative value of end cap load reduction. As in prior pull out tests, there was considerable scatter in the pull test data. The highest pull force recorded at 0.25 inch cross head displacement was [ ]$^{a,c,e}$ lbf, and the lowest pull force recorded at 0.25 inch cross head displacement was [ ]$^{a,c,e}$ lbf. Monte Carlo simulation was then used to determine a 5/50 value (i.e., the lower 95% bound) of the pull test data.

The Monte Carlo simulations used the pull test data to establish means and standard deviations for the pull forces that were observed. Two sets of data for each of three tube diameters (0.688 inch, 0.750 inch, and 0.875 inch) were provided: One considered the 13 in. expansion lengths only and the other considered all expansion lengths (13, 15 and 17 inches) combined. Seven distributions were used: 1) A truncated (at 0) normal distribution, 2) a lognormal distribution, 3) an Erlang distribution, 4) a Gamma distribution, 5) an inverse Gaussian distribution, 6) a Pearson Type V distribution, and 7) a Weibull distribution. All except the truncated normal were chosen because their domains range from 0 to + infinity, their domains are continuous, and their fitting parameters for the means and standard deviations used were within their allowable values. One hundred thousand iterations were run for each simulation, and the 5/50 values of pull force recorded for each distribution. The most conservative result, [ lbf]$^{a,c,e}$, came from the simulation that used the Weibull distribution, and this number is very consistent with the lowest observed pull test datum. Note that the Weibull distribution is widely recommended to model distributions in lieu of a truncated normal distribution. The figure below illustrates the results of the Monte Carlo sampling based on the Weibull distribution of the test data. Complete details of the above analysis can be found in Reference RAI20-2.

The recommended end cap load reduction is [ ]$^{a,c,e}$ lbf.

[ ] a,c,e

(Figure corresponding to the Monte Carlo simulation using a Weibull distribution for the Model F SG data, using the 13 inch expansion length only. The 5/50 value of pull force is [ ]$^{a,c,e}$ lbf.)

F. Application of Residual Contact Load

The H* results in Figure 8-5 of WCAP-17071-P, WCAP-17072-P, WCAP-17091-P and WCAP-17092-P show that H* is sensitive to the variations in the coefficient of thermal expansion (CTE) of the tube ($\alpha_T$) and the tubesheet ($\alpha_{TS}$). The reports also show that H* is not significantly sensitive to variations in the Young's modulus (E) of the tube or the tubesheet. The results in Figure 8-5 in WCAP-17071-P, WCAP-17072-P, WCAP-17091-P and WCAP-17092-P also demonstrate that the worst case trend in the variation of the thermal expansion coefficients is when the $\alpha_T$ is decreasing and $\alpha_{TS}$ is increasing. In other words, H* increases the most when the coefficients of thermal expansion are varied to reduce the contact pressure between the tube and the tubesheet due to thermal growth.

It is possible to reduce the order of the problem (i.e., reduce the number of dimensions involved in the sensitivity study) given the knowledge of which values and directions of variation in CTE are most important to the problem. Figures RAI10-1 and RAI10-2 show the combinations of $\alpha_T$ and $\alpha_{TS}$ that are most likely to produce a worst case H* value. The values of CTE standard deviations for both the tube and tubesheet are combined into an effective variable using the following relationship:

$$\alpha_{srss} = \sqrt{(-\sigma_{\alpha T})^2 + (\sigma_{\alpha TS})^2}$$

The possible variation in sign of either CTE standard deviations is not included in this equation because the only values of interest occur when the tube CTE variation is negative relative to the mean and the tubesheet CTE variation is positive relative to the mean. This reduced form of variation in CTE is then used to compare the change in H* due to the application of residual pre-load between the tube and the tubesheet due to the installation and hydraulic expansion of the tube.

There are multiple ways to achieve the same value of $\alpha_{srss}$. For example, a TS CTE variation of +5$\sigma$ about the mean and a tube CTE variation of -5$\sigma$ about the mean are each equal to a combined $\alpha$ of 5 (assuming only one is non-zero). Likewise, a combination of tube and TS CTE variations of -3/+4 and -4/+3 will also yield an $\alpha$ of 5. However, the net change in H* with respect to the material properties are very similar for a single value of $\alpha_{srss}$ regardless of values of its component parts. In cases where there are multiple possibilities for a unique value of $\alpha_{srss}$, the combination of TS and tube CTE that produced the smallest reduction in H* was used. Figure RAI20-8 shows the multiple curves that were used to create the surface seen in RAI20-9.

Hydraulic expansion of the tube into contact with the tubesheet tube bore introduces a pre-load that must be overcome before the tube can translate within the tubesheet tube bore. This means that in addition to the pull out resistance that a tube develops due to internal pressure, thermal growth, etc., the pull out resistance of the tube due to the hydraulic expansion must also be overcome in order for the tube to freely translate within the tube bore. However, the hydraulic expansion process has only a small effect on the development of contact pressure between the tube and the tubesheet compared to that developed due to operating pressure and temperature. Therefore, the installation effect, termed residual contact load (RCL), is included as a reduction of the applied end cap load. Recall that the end cap loads are based on the mean +2$\sigma$ tubesheet bore diameter and are thus very conservative.

The reduction in end cap load, for the $i^{th}$ value of pull out resistance due to installation effects is:

$$P_i = \text{End Cap Load} = n\Delta p \pi r_o^2 - DL - RCL_i$$

Where,

$n$ is the applicable safety factor for the SG operating condition based on the SIPC,

$\Delta p$ is the primary to secondary pressure differential,

$r_o$ is the outside tube radius,

*DL* is the dead load of the tube straight leg above the top of the tubesheet and *RCL* is the value of installation pre-load determined from test results.

The minimum pull out force from section F above, [ ]$^{a,c,e}$ lbf, was used. The dead weight of the straight leg portion of the tube above the tubesheet was also included because it also provides a resistance to tube pull out. The dead weight of the straight legs of the tubes varies between [ ]$^{a,c,e}$ and [ ]$^{a,c,e}$ lbs depending on the length of the tube straight leg; an average value of [ ]$^{a,c,e}$ lbs was used.

As an example, for the NOP Low $T_{avg}$ condition at Millstone Unit 3, the end cap load due to the pressure acting on the tube is [ ]$^{a,c,e}$ lbf. Assuming the minimum value of pull out force from the test data and an average dead weight of the tube straight leg, the applied end cap load that must be balanced by the distribution of contact pressure between the tube and the tubesheet is equal to [ ]$^{a,c,e}$ lbf – [ ]$^{a,c,e}$ lbf – [ ]$^{a,c,e}$ lbf, or [ ]$^{a,c,e}$ lbf.

Using the RCL to reduce the end cap load on the tube has been shown to be conservative in a direct comparison with the alternative method, that is, converting the pull out force to a residual contact pressure and including it in the integration for H*. Further, reduction of the applied load does not affect the contact pressure distribution between the tube and the tubesheet. For instance, if there was a combination of material properties and operating conditions that resulted in a very small or zero value of contact pressure for some portion of the tube below the top of the tubesheet, the application of RCL as a reduction of applied load does not change the predicted contact pressure. The first point of positive contact between the tube and the tubesheet is still determined based on the structural analysis of the tubesheet. An additional benefit from applying the RCL as a reduction to the applied end cap load is that there is no need to develop a distribution of the residual effect of the tube installation as a function of elevation in the tubesheet. The test results can be directly used to determine the pre-load on the tube.

A value of H* is determined for any value of RCL for the limiting SG operating condition at the limiting TS radius and sector in the bundle. The process for determining the H* value is shown in the following flow chart.

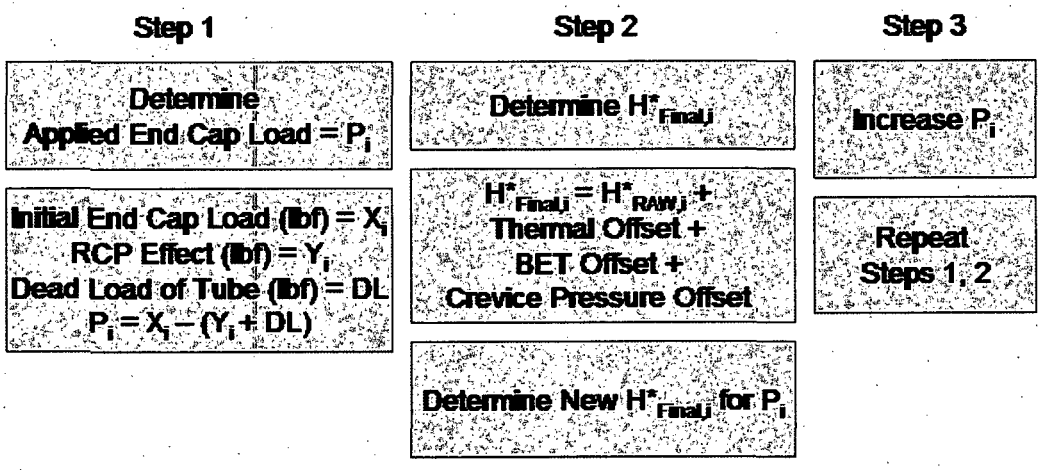


The result of this process is a surface of the response in H* to changes in RCL and $\alpha_{srss}$ the square root of the sum of squares of the specific variations in CTE from one MC simulation). If the values for RCL are normalized to an assumed value, say [ ]$^{a,c,e}$ lbf, and the values of H* are taken as the change in H* relative to the value of H* with an RCL of zero, the result is a non-dimensional surface that can be used in conjunction with a Monte Carlo analysis to determine the reduction in H* due to the inclusion of RCL. Figure RAI20-9 is a surface plot of the change in the Model F H* values as a function of RCL and $\alpha_{srss}$. Figure RAI20-10 is a surface plot of the change in the Model D5 H* values as a function of RCL and $\alpha_{srss}$.

Figure RAI20-9 and RAI20-10 illustrate that the effect of including the RCL as a reduction in the applied tube end cap load is dependent on both the H* value and the material parameters. This is a logical result because if H* is small (correlated to a small value of $\alpha_{srss}$) then the effect of RCL should also be small because there is enough contact pressure to maintain equilibrium with the load on the tube regardless of the value of RCL. However, if H* is large, because of some combination of material parameters or operating conditions that produce less contact pressure between the tube and the tubesheet, then the presence of any value of RCL has a much larger effect on H*. For example, in Figure RAI20-8, assuming an RCL ratio of 1 (RCL ~[ ]$^{a,c,e}$ lbf) with an $\alpha_{srss}$ of 0 results in a very small correction to the final H* distance on the order of [ ]$^{a,c,e}$ inch. However, if the RCL ratio is equal to 1 and $\alpha_{srss}$ is equal to 5, the change in H* is 2 or more inches, or a factor of 4 greater.

The effects of residual contact pressure (RCP) are implemented in the extreme-value simulation model using a functional representation of the developed steam generator-specific data described above. The function describes the correction term ( $\Delta H^*$ ) in terms of two variables:

$$\Delta H^* = G(\text{ RCL, Alpha })$$

Where:

RCL = Residual contact load
Alpha = Effective thermal expansion coefficient

A typical description of this surface is shown in Figure RAI20-8. As can be seen from the figure, the behavior of the function is somewhat complex. The value of the function generally increases with both independent variables which makes some simplification possible based on a conservatively low estimate of one of the variables.

A lower limit constant value of RCL was chosen, in part to assure a more robust computational behavior in the implementation of the RCL effects modeling. The value cited in the response to part F of this RAI corresponds to a RCL ratio of approximately 1.0. Figure RAI20-11 shows the resulting $\Delta H^*$ as a function only of Alpha. This and corresponding functions for each steam generator class, were implemented in the full simulation model.

The actual implementation into the simulation model was straightforward. Since the RCL correction is subtractive, the computation of Alpha and $\Delta H^*$ is performed directly after the computation of $H^*$ within the simulation. The computation is performed for all tube/tubesheet combinations in the entire simulation process. The reduction in the computed extreme values of $H^*$ is typically on the order of 1-2 inches, and is steam generator–specific.

It is important to note that the change in $H^*$ due to the crevice pressure adjustment, thermal offset and BET is already included in the analysis. The distribution of the crevice pressure adjustment shown in Figure 8-1 of the $H^*$ reports is not required in this instance. That is because the reduction of the end cap load changes how the $H^*$ value will react to a change in contact pressure distribution. So it is necessary to incorporate the change in $H^*$ due to the RCL reduction of the end cap load with the crevice pressure adjustment to produce a net change in $H^*$ using consistent methods. Therefore, the result of using the RCL surface to determine the change in $H^*$ is the net effect of all adjustments to $H^*$ and no further corrections are required.

Table RAI2-05(c) summarizes the effects of the application of residual pull out load (RCL) on the value of $H^*$. When the 5/50 pull out force from the test data is applied using the Monte Carlo approach that samples from Figure 8-5 in the reports and also from the RCL correction surface discussed above, the values of $H^*$ are reduced approximately 1 to 2 inches for all affected models of SGs. The resulting values of $H^*$ for the Model F and Model D5 SGs are further reduced by application of the updated NOP temperature distribution correction factor. As can be seen from Table RAI20-5, the recommended values of $H^*$ for the respective SGs in the applicable reports exceeds the values determined when the conservative factors inherent in the recommended values are considered in the analysis.

G. Summary and Conclusions

The recommended values of H* for the different models of SGs as provided in the respective reports (WCAP-17071-P [Model F], WCAP-17072-P [Model D5], WCAP-17091-P [Model 44F] and WCAP-17092-P [Model 51F]) were based on very conservative assumptions. Additional analysis, using Monte Carlo techniques and the variables interaction surfaces defined in Figure 8.5 of the reports, was performed to quantify the conservatism of these assumption with regard to the recommended values of H* for the different models of SGs. Four principal conservatisms were evaluated:

1. The number of tubesheets was limited to a number less than the number of tubes in the bundles of the respective SG models. The total population of SGs among the H* candidate plants is 60 including 4 different models of SGs. The number of tubesheets simulated for each SG was limited to 10,000.

2. Instead of assuming that all tubes in the bundle are located at the single worst case position that defines the recommended value of H*, the bundles were divided into sectors. This approach retains significant conservatism because the maximum value of H* in each sector was used for the analysis and the limiting interaction variances were applied to all sectors. It is noted that all sectors considered are located in the limiting azimuthal sector of the tubesheet as discussed in Section 6.2.3 of the reports.

3. The conservative adder for NOP tubesheet thermal distribution was re-evaluated by including the thermal distribution directly in the structural analysis. The resulting adders to H* are realistic values that reflect the actual response of the tubesheet structure to the applied thermal distribution. This applies only for the Model F and Model D5 SGs because the updated thermal correction factor is already included in the recommended H* values for the Model 44F and 51F SG. Modification of the thermal distribution factors does not change that the NOP conditions are the limiting conditions that determine the value of H*.

4. Based on pull out tests performed during the H* development, the effect of the minimum measured pull out forces at 0.25 inch of tube travel on the values of H* were evaluated. The pull out force data was applied directly as a reduction of the applied loading instead of utilizing an intermediate conversion of pull out force to contact pressure. This approach is more direct, and its specific application is conservative because the 5/50 value of pull out force was used. In reality, much greater values of pull out force were demonstrated in the tests at 0.25 inch travel. Still greater pull out forces were observed during the tests for greater values of tube travel, even exceeding the limiting applied design loads for H*. Therefore, the application of the 5/50 value of pull out force from the tests is conservative.

After addressing the above factors, the final values of H* are significantly less than the values recommended for all affected models of SGs. Therefore, the recommended values of H* for each of the models of SG are shown to be conservative.

RAI#20 References:

RAI20-1 LTR-SGMP-09-92;"Tubesheet Sector Definition for H* Revised Probabilistic Analysis," July 10, 2009.

RAI20-2 LTR-SGMP-09-98, "H* Pull Test Program Summary," July 27, 2009.

**Figure RAI20-1**
**Model F**

a,c,e

**Figure RAI20-2**
**Model D5**

a,c,e

**Figure RAI20-3**
**Model 44F**

a,c,e

[ ]

**Figure RAI20-4**
**Model 51F**

a,c,e

[ ]

**Figure RAI20-5**
**Monte Carlo Simulation Process**

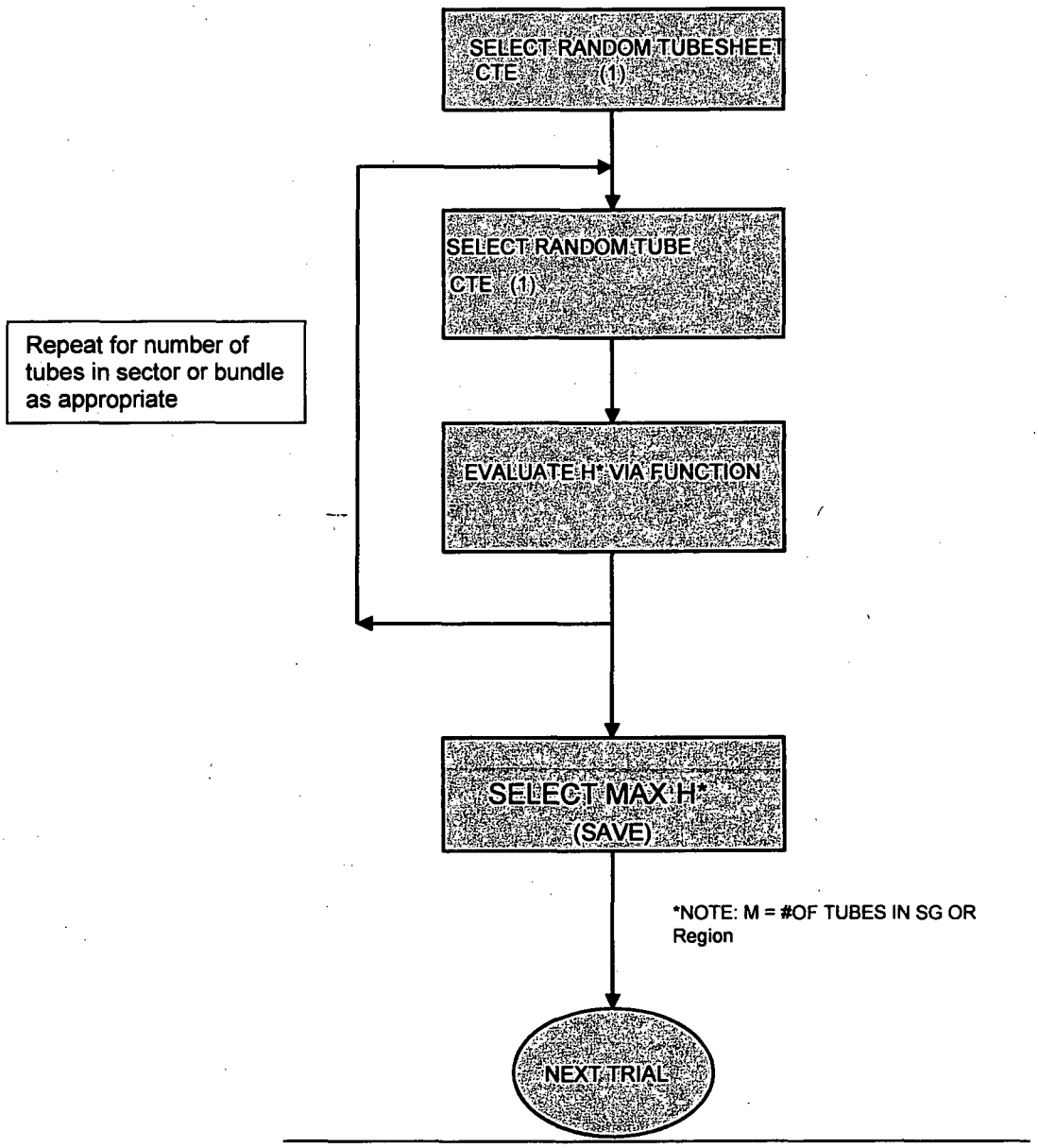

**Figure RAI20-6**
**Model F: Interaction Profiles for Sector-Base Sampling**

a,c,e

[ ]

**Figure RAI20-7**
**Model D: Interaction Profiles for Sector-Base Sampling**

a,c,e

[ ]

**Figure RAI20-8**

**$\Delta H^*$ for Various Values of $\alpha_{srss}$ and RCL Ratio**

($a = \alpha_{srss}$, $RCL_{ref}$ = 800lbf)

a,c,e

[ ]

**Figure RAI20-9**
**Model F Response Surface for the Change in H* as a Function of RCL and $\alpha_{srss}$**

a,c,e

[ ]

**Figure RAI20-10**
**Model D5 Response Surface for the Change in H* as a Function of RCL and $\alpha_{srss}$**

a,c,e

[ ]

**Figure RAI20-11**
**Change in H* as a Function of $\alpha_{srss}$**

a,c,e

[ ]

**Table RAI20-1**
**Model F SG Sector Populations**

| Model F | | | | | | | | | |
|---|---|---|---|---|---|---|---|---|---|
| TS Radius | 0-11 | 11-17 | 17-23 | 23-29 | 29-35 | 35-41 | 41-47 | 47-53 | 53-60 |
| Max Mean H* | | | [ ]a,c,e | | | | | | |
| Max Mean H*Factor | [ | | | | | | | | ] |
| Number of Tubes | [ | | | | | | | | ] |

a,c,e

**Table RAI20-2**
**Model D5 SG Sector Populations**

| Model D5 | | | | | | | | | |
|---|---|---|---|---|---|---|---|---|---|
| TS Radius | 0-6 | 6-12 | 12-18 | 18-24 | 24-30 | 30-36 | 36-42 | 42-48 | >48 |
| Max Mean H* | | | | | [ ]a,c,e | | | | |
| Max Mean H*Factor | [ | | | | | | | | ] |
| Number of Tubes | [ | | | | | | | | ] |

a,c,e

**Table RAI20-3**
**Model 44F SG Sector Populations**

| Model 44F | | | | | | | | | |
|---|---|---|---|---|---|---|---|---|---|
| TS Radius | <9 | 9-15 | 15-21 | 21-27 | 27-33 | 33-39 | 39-45 | 45-51 | >51 |
| Max Mean H* | | | [ ]a,c,e | | | | | | |
| Max Mean H*Factor | [ | | | | | | | | ] |
| Number of Tubes | [ | | | | | | | | ] |

a,c,e

**Table RAI20-4**
**Model 51F SG Sector Populations**

| TS Radius | | <9 | 9-17 | 17-24 | 24-32 | 32-41.85 | 41.85-52.52 | >52.52 |
|---|---|---|---|---|---|---|---|---|
| Max Mean H* | | | | [ ]a,c,e | | | | |
| Max Mean H*Factor | | [ | | | | | | ] |
| Number of Tubes | | [ | | | | | | ] |

a,c,e

**Table RAI20-5**
**Results of Monte Carlo Sampling and Valuation of Conservatism**

| SG Model | Report Case S-2 | | | Surface Sampling from Figure 8-5 of the Report(s) with Limited Number of Tubesheets and Sector Based Approach | | |
|---|---|---|---|---|---|---|
| | 95/50 (inch) | Pcrev (inch) | Final H*(inch) | 95/50 (inch) | Pcrev | Final H* |
| F | | | 11.2 | | | |
| D5 | | | 13.8 | | | |
| 44F | | | 13.31 | | | |
| 51F | | | 13.14 | | | |

a,c,e

(a) Sampling from Interaction Surface Figure 8-5

| SG Model | H* After Surface Sampling | Correction for NOP Thermal Distribution | | | Surface Sampling, Limited Tubesheets Corrected for NOP Thermal Offset | | |
|---|---|---|---|---|---|---|---|
| | 95/50 H*(inch) | Original (inch) | Revised (inch) | | 95/50 H*(inch) | Pcrev (inch) | Final H*(inch) |
| F | | | | = | | | |
| D5 | | | | = | | | |
| 44F | | | | = | | | |
| 51F | | | | = | | | |

a,c,e

| SG Model | Surface Sampling from Figure 8-5 of the Report(s) with Limited Number of Tubesheets | □H* for Minimum Pull Out Force (inch) | Final H* After Including Minimum Pull Out Force | Correction for NOP Thermal Distribution | Final H* (inch) |
|---|---|---|---|---|---|
| | 95/50 (inch) | NA | (95/50) (inch) | (inch) | (95/50) (inch) |
| F | | | | | |
| D5 | | | | | |
| 44F | | | | | |
| 51F | | | | | |

a,c,e

(c) Adjustment for Residual Contact Pressure

Notes:

1. The value of H* before correction for $P_{crev}$ is used because the interaction surface is based on the H* value without the $P_{crev}$ adjustment.

***There are a number of utility specific RAIs with numbers in the range of RAI 21 through 23, depending on the specific utility. The responses to utility-specific RAIs are provided under separate cover by the utilities.***

| | | |
|---|---|---|
| ***RAI*** | *Vogtle* | *24. Reference 1, Page 9-6, Section 9.2.3.1: The feedwater line break heat-up transient is part of the plant design and licensing basis. Thus, it is the NRC staffs position that H* and the "leakage factors," as discussed in Section 9.4, should include consideration of this transient. Explain why the proposed H* and leakage factor values are conservative, even with consideration of the feedwater line break heat-up transient.* |
| | *WCGS* | *24. Reference 1, page 9-6, Section 9.2.3.1: The FLB heat-up transient is part of the plant design and licensing basis. Thus, it is the staff's position that H* and the "leakage factors," as discussed in Section 9.4, should include consideration of this transient. Explain why the proposed H* and leakage factor values are conservative, even with consideration of the FLB heat-up transient.* |
| | *B/B* | *23. Reference 1, Page 9-6, Section 9.2.3.1: The FLB heat-up transient is part of the plant design and licensing basis. Thus, it is the NRC staffs position that H* and the "leakage factors," as discussed in Section 9.4, should include consideration of this transient. Explain why the proposed H* and leakage factor values are conservative, even with consideration of the FLB heat-up transient.* |
| | *CPSES* | *24. Reference 1, page 9-6, Section 9.2.3.1: The FLB heat-up transient is part of the plant design and licensing basis. Thus, it is the NRC staff's position that H* and the "leakage factors," as discussed in Section 9.4, should include consideration of this transient. Please explain why the proposed H* and leakage factor values are conservative, even with consideration of the FLB heat-up transient.* |
| | *Seabrook* | *24. Reference 1, Page 9-6, Section 9.2.3.1: The feedwater line break heat-up transient is part of the plant design and licensing basis. Thus, it is the staff's position that H* and the "leakage factors," as discussed in Section 9.4, should include consideration of this transient. Explain why the proposed H* and leakage factor values are conservative, even with consideration of the feedwater line break heat-up transient.* |

Response:

Radiological consequences are a function of the source term and activity transport.

- Source term refers to the activity available for release. This is controlled by the Tech Specs on primary and secondary activity and the iodine spike

considerations required by the NRC. Fuel damage is not expected for either the SLB or the FLB. As a result, the source term would be the same. This is the case for the H* plants under consideration.

- Activity transport is dependent upon initial locations of the activity and the mechanism for transport that are applicable. For both the SLB and the FLB events, the dose calculation would use the Tech Spec leakage rate for tube leakage. For both the SLB and FLB events, the secondary break would be assumed to occur outside containment such that the faulted SG releases would occur directly to the atmosphere. As a result, the activity transport would be the same.

Therefore, calculation of the dose consequences for the SLB event would be identical to the calculations that would be made for a FLB event. In this subject, the item that is addressed by the H* program is to define a criterion such that the Tech Spec tube leakage is adequately bounding for both the FLB and SLB. The approach that is used is to define single values for a conservative temperature and conservative pressure differential for the determination of the leakage rate. For the purposes of the dose calculation, these single values are effectively assumed both to be simultaneously occurring and to be continuous for the duration of the calculation. In the dose calculations, these leakage conditions are assumed to last anywhere from multiple hours to multiple days. In some cases, the timeframe is based on allowing for plant cooldown to 212°F which would also require depressurization of the RCS and, therefore reducing the severity of conditions contributing to the tube leakage. However, as noted above, the dose calculations do not consider a more realistic set of conditions for tube leakage.

With respect to temperature transients, a review of the steam generator design transients and the FSAR safety analyses determined that they are not appropriate for defining a temperature basis for the leakage calculations. Those calculations are focused on different criteria and include assumptions which would be overly conservative and operationally limiting for the H* program. For secondary side breaks occurring outside containment, reasonable assumptions would result in a much greater cooling capability of the steam generator secondary side inventory in comparison to FSAR safety analyses. Moreover, based on engineering judgment, a more realistic time-dependent leakage for these events, would result in dose consequences that are less than those reported in the UFSAR under the current licensing basis for both a postulated SLB and FLB event (including a FLB heatup event) due to the reduction in pressure across the tubes and tubesheet that occurs over the long term duration of the accident that is not currently accounted for in the dose analysis. This effect has not been quantified nor does it need to be. It is simpler to define a reasonable peak temperature to use as a basis for the duration of the dose calculation. As identified in WCAP-17071-P and WCAP-17072-P, Westinghouse believes that, with assumptions consistent with an outside containment break, and considering operator actions that are consistent with current Emergency Operating Procedures (EOPs), the no-load condition for a plant is a reasonable condition to use as the basis of the primary to secondary

leakage. The EOPs, for an event which results in a Safety Injection, provide for reduction/termination of safety injection flow and for initiation of cooldown and depressurization of the reactor coolant system to the point that the RHR system can be placed in operation for continued cooling of the RCS. These actions will significantly reduce the pressure and temperature of the RCS to conditions less than the limiting conditions proposed for use in the H* calculations. The cooldown is initiated by releasing steam from the steam generators by using the systems that are available at the time. The steaming of the steam generators provides the additional benefit of increasing the available AFW flow injection due to a reduced pressure that the AFW pumps have to overcome. Either by considering a reduction in dose consequences due to a more realistic time dependent leakage for these events or by considering that the FLB event is best represented as a cooldown event, it is concluded that no change is required to the leakage factors for the Model F and D5 SGs as reported in WCAP-17071-P and WCAP-17072-P.

However, the NRC staff has pointed out that the "figure of merit" in the technical specification performance criterion is "the leakage rate assumed in the accident analysis" and that a FLB heatup event is part of the current licensing basis for certain plants in the H* fleet. Therefore, to ensure that there is sufficient margin between the accident leakage and operational leakage during a postulated FLB as required by the plant Technical Specifications and to ensure that the implementation of the H* criterion remains within the current licensing basis, an adjustment to the leakage factors provided in Table 9-7 of WCAP-17071-P and WCAP-17072-P has been made that accommodates the design specification FLB heatup event. As noted above, the use of temperatures from this transient is judged to be non-realistic and overly conservative. As described in WCAP-17071-P and WCAP-17072-P, for the Model F SGs, the FLB design transient represents a double–ended rupture of the main feedwater line concurrent with both a Station Blackout (loss of main feedwater and reactor coolant pump coastdown) and Turbine Trip. For the Model D5 SGs, the maximum RCS temperature of 670°F exceeds the saturation temperature which is not predicted to occur by the worst case Chapter 15 Safety Analysis Transient response.

Because a FLB heat-up event would result in an increase in primary-to-secondary leakage due to the reduction in viscosity of the reactor coolant, the extent of temperature increase must be quantified to address the impact on radiological consequences for the H* plants with Model F and Model D5 steam generators. Referring to references 9-12 and 9-13 of WCAP-17071-P and WCAP-17072-P, the maximum temperature rise for a Model F SG is less than 6.5°F above the normal operating hot leg temperature (approximately 630°F). For the Model D5 steam generator, the maximum increase in temperature is 50°F above the normal operating hot leg temperature (approximately 670°F). This would require a negligible increase in leakage factor for the Model F SGs reported in Table 9-7 (to a maximum of 2.05 from 2.03) and a slight increase in leakage factors reported for the Model D5 steam generators (to a maximum of 2.31 from 2.03).

The maximum temperature rise for a Model F SG is 66°F above the normal operating cold leg temperature (to approximately 620°F). For the Model D5 steam generator, the maximum increase in cold leg temperature is 120°F above the normal operating cold leg temperature (to approximately 670°F). This would require a maximum increase in leakage factor of 1.23 times the factors provided for the individual Model F SGs in Table 9-7 (to a maximum value of 2.50) and a maximum increase in leakage factor of 1.63 times the factors provided for the individual Model D5 steam generators to a maximum value of 3.16. The leakage factor for the cold leg is limiting for a FLB heat-up event and should be incorporated into the reporting requirements for the plant technical specifications.

Revised versions of Tables 9-1 and 9-7 from WCAP-17071-P and WCAP-17072 -P are provided in this RAI response to reflect the potential increase in temperature that may occur during a postulated FLB event.

Finally, the feedwater line break heat-up transient definition is not a concern for the H* structural analysis. The SIPC requirement for calculating the end cap load during the faulted condition (1.4DP) during the feedwater line break condition does not exceed the end cap load applied to the tubes during NOP (3.0DP). In fact, the applied end cap load during feedwater line break, regardless of whether it is a heat-up or cool down feedwater line break, is several hundred pounds less than the end cap load applied during normal operating conditions. Therefore, normal operating conditions are bounding for the structural determination of H* in all cases. Please refer to Section 5 and Section 6 in the WCAP 17071-P and WCAP-17072-P for a discussion of the calculated end cap loads and the contact pressure results for the feedwater line break condition.

**Table RAI24-1**
**Revised Table 9-1 Reactor Coolant System Temperature Increase Above Normal Operating Temperature Associated With Design Basis Accidents**

(References 9-12 and 9-13)

a,c,e

| SG Type | Steam Line/Feedwater Line Break(1) | | Locked Rotor (Dead Loop) | | Locked Rotor (Active Loop) | | Control Rod Ejection | |
|---|---|---|---|---|---|---|---|---|
| | SG Hot Leg (°F) | SG Cold Leg (°F) | SG Hot Leg (°F) | SG Cold Leg (°F) | SG Hot Leg (°F) | SG Cold Leg (°F) | SG Hot Leg (°F) | SG Cold Leg (°F) |
| | | | | | | | | |
| | | | | | | | | |
| | | | | | | | | |
| | | | | | | | | |

(1) The postulated SLB does not result in a temperature increase above normal operating conditions as the SLB is a cooldown transient, only the postulated FLB can result in a heatup event dependent upon accident analysis assumptions. The postulated FLB is not part of the licensing basis for plants with Model 44F and Model 51F SGs.

## Table RAI24-2
## Revised Table 9-7 Final H* Leakage Analysis Leak Rate Factors (Revised)

| Transient | SLB/FLB | | | Locked Rotor | | | | Control Rod Ejection | | | |
|---|---|---|---|---|---|---|---|---|---|---|---|
| Plant Name | FLB-SLB/NOP ΔP Ratio (High $T_{avg}$)[2] | VR[3,4] @ 2642 psig | SLB/FLB Leak Rate Factor(LRF) | LR/NOP ΔP Ratio | VR[3] @ 2711 psia | Leak Rate Factor (LRF) | Adjusted LR LRF[1] | CRE/NOP ΔP Ratio | VR[3] @ 3030 psia | Leak Rate Factor (LRF) | Adjusted CRE LRF[1] |
| Byron Unit 2 and Braidwood Unit 2 | 1.93 | 1.61 | **3.11** | | | | | | | | |
| Salem Unit 1 | 1.79 | 1.21 | **2.16** | | | | | | | | |
| Robinson Unit 2 | 1.82 | 1 | **1.82** | | | | | | | | |
| Vogtle Unit 1 and 2 | 2.02 | 1.23 | **2.48** | | | | | | | | |
| Millstone Unit 3 | 2.02 | 1.23 | **2.49** | | | | | | | | |
| Catawba Unit 2 | 1.75 | 1.52 | **2.65** | | | | | | | | |
| Comanche Peak Unit 2 | 1.94 | 1.63 | **3.16** | | | | | | | | |
| Vandellos Unit 2 | 1.97 | 1.22 | **2.41** | | | | | | | | |
| Seabrook Unit 1 | 2.02 | 1.23 | **2.49** | | | | | | | | |
| Turkey Point Units 3 and 4 | 1.82 | 1 | **1.82** | | | | | | | | |
| Wolf Creek | 2.03 | 1.23 | **2.50** | | | | | | | | |
| Surry Units 1 and 2 | 1.80 | 1 | **1.80** | | | | | | | | |
| Indian Point Unit 2 | 1.75 | 1 | **1.75** | | | | | | | | |
| Point Beach Unit 1 | 1.73 | 1 | **1.73** | | | | | | | | |

a,c,e

1. Includes time integration leak rate adjustment discussed in Section 9.5.
2. The larger of the ΔP's for SLB or FLB is used.
3. VR – Viscosity Ratio
4. VR – Viscosity Ratio in SG cold leg during a postulated FLB heatup event

# APPENDIX A
# SUMMARY OF 2008-2009 PULL OUT TEST PROGRAM IN SUPPORT OF H*

**Abstract**

Steam generator tubes made of Alloy 600 (A600) were hydraulically expanded in AISI 1018 cold rolled, carbon steel, cylindrical collars, which simulate the steam generator tubesheet, and then pulled by an MTS machine out of the collars in order that tube-to-tubesheet joint (hereafter referred to as "joint" or "the joint") strength might be measured. Nine tubes from each of Model F, Model D5, and Model 44F tubes were tested for pull out resistance, three at each expansion length (13 inches, 15 inches, and 17 inches). The pull out test parameters were established so that the results can be considered to be prototypic of the as-built condition of the steam generators within the H* fleet (i.e., the test specimens were designed and manufactured to be within the manufacturing tolerances for dimensional variations, material properties, and process control parameters for the H* fleet steam generator tube joints).

The pull force capacity associated with 0.25 inch tube displacement relative to the tubesheet ranged from approximately [ ]$^{a,b,c}$ lbf to approximately [ ]$^{a,b,c}$ lbf. The values for the maximum pull force ranged from approximately [ ]$^{a,b,c}$ lbf to approximately [ ]$^{a,b,c}$ lbf within a maximum relative displacement of 2.02 inches, regardless of the tube outside diameter or hydraulic expansion length[10].

Monte Carlo simulations were performed in order to better define a 5/50 value of pull force, which is based on the presence of residual contact pressure, for use in the H* analysis. The minimum 5/50 value of the pull force has been observed to be [ ]$^{a,b,c}$ lbf, and this corresponds very well to the lowest recorded pull force from the testing.

**Introduction**

H* (pronounced "H star") is the length of hydraulically expanded steam generator tube that must remain intact within the tubesheet in order for the joint to resist pull out and leakage due to normal operating or accident conditions. The basis of the H* program is such that residual contact pressure between the tube and the tubesheet is not considered in the structural or leakage calculations. Hence, any indication of joint strength from test program data is a measure of conservatism contained in the H* analysis.

Westinghouse commenced a test program in which steam generator tubes were hydraulically expanded in cylindrical collars representing the tubesheet and pulled to measure joint strength. There were no tack expansions, hard rolled expansions, or welds to consider. Initially, the H* program applied to Model F steam generators, but it has been expanded to include Model D5, Model 44F, and Model 51F steam generators. The following sections of this document summarize the results of this test program.

## Experimental

*Materials*

Alloy 600 tubes representing those from Model F, Model D5, and Model 44F steam generators were cut to seventeen, nineteen, and twenty-one inch lengths. The Model F steam generator tube was taken from Heat NX7368 and is believed to be mill annealed. The Model D5 and Model 44F steam generator tubes were taken from Heats 2645 and 752570, respectively, and both are in the thermally treated condition. The chemical analyses for these materials are contained in Table 1 and the mechanical properties are contained in Table 2. Note that the mechanical properties listed in Table 2 are from the providers' certifications and from testing done at Industrial Testing Laboratory Services (ITLS). The latter tests were done according to ASTM E8-08 [1].

The cylindrical collars representing the tubesheet were cut to fifteen, seventeen, and nineteen inch lengths from AISI 1018 cold-rolled, carbon steel. The chemical analysis and mechanical properties of Heat 777553 are contained in Tables 3 and 4, respectively. It should be noted that the outer diameters of the collars were chosen to be [ ]$^{a,c,e}$ times the outer diameter of the tubes so that the stiffness of the actual tubesheet plate is correctly represented. This ratio is based on the work of Middlebrooks et al. [2].

The list of tube and collar pairings is presented in Table 5. The indices are to be read as follows: the first two indices refer to the overall length of the tube or collar, the second three indices refer to the nominal OD of the tube or the nominal ID of the collar, and the last two indices refer to the sample number. The "A" suffix refers to a second manufacture of the same sample. It should be noted that two of the tests done were originally planned to be diagnostic in nature. The collars were rebored so that they would contain an inner diameter surface finish of 250 micro-inch rms max. vice an engineered finish of 250 micro-inch rms. These collars were from Heat 730492, and its properties are also contained in Tables 3 and 4.

*Pre-Expansion Measurements*

The inner diameters of the collars were measured by the vendor (Tooling Specialists, Inc., Latrobe, PA) at distances corresponding to 25%, 50%, and 75% of the length of the collar, relative to the serialized end. Two measurements, ninety degrees apart, were made with an intramic at each location, and the two values at each location were then averaged. Surface roughness measurements were also made by the vendor at the 25% and 75% distances using a profilometer. Lack of an extension device for the profilometer did not permit roughness measurements at the 50% distance.

After being cut, the inner and outer diameters of the A600 tubes were measured by an intramic and the surface roughness of the outer diameters were measured with a profilometer at Westinghouse RRAS (R. Fetter). The diameter measurements were made, relative to the non serialized end, at distances that overlap those made in the collars. Thus, the 25%, 50%, and 75% distances correspond to those percents of the collar's length, not the tube's length. The

inner and outer diameters were also measured at two points for each distance, ninety degrees apart, and the two values were averaged.

*Hydraulic Expansion*

The tubes were inserted in the collars such that the non serialized end of the tube was flush with the serialized end of the collar. Thus, the serialized end of the tubes protruded from the collars by two inches. The tube/collar assemblies were then inserted on an O-ring mandrel, which was connected to a screw drive pressurizing system. The tube/collar assemblies were pressurized to a nominal pressure of [ ]$^{a,c,e}$ psi per Process Specification 81013RM, Revs. 4 through 10 applicable [ ]. The nominal expansion pressure was typically exceeded, but the excess was less than [ ]$^{a,c,e}$ psi, which is within the tolerance of the equipment ([ ]$^{a,c,e}$ psi). This work was performed at Westinghouse's Waltz Mill facility by M. Gallik and A. Stett. The details of the tube expansion test plan are contained in [4].

*Post-Expansion Measurements*

After the hydraulic expansions were completed, measurements of the tubes' inner diameters were again made with an intramic by Westinghouse RRAS (R. Fetter), and eddy current measurements of individual tube/collar assemblies were performed by Westinghouse with the 3-coil +point and standard bobbin coil probes (R. Pocratsky). Once the measurements were complete, the end caps were welded to the tubes at their serialized ends. The tube/collar assemblies with the end caps welded on are shown in Figures 1 through 9.

*Heat Treatment*

Real tubesheet Z-channels are given a post-weld heat treatment (PWHT) with an electric "belt" wrapped around the channel. In order to simulate that PWHT, the tube/collar assemblies were heat treated in air at nominally [ ]$^{a,c,e}$ °F for nominally 3 hours in a Blue M furnace, Model B-2730-Q. This was accomplished at Westinghouse's Churchill site (A. Neville). The actual PWHT temperature applied to the Z-channel is 1150°F. However, it was determined [5] that [ ]$^{a,c,e}$ °F is higher than the vast majority of the tubes will experience by the PWHT.

*Instrumentation*

Prior to testing, the exposed ends of the tubes were fitted with two 350 ohm, quarter bridge strain gauges. Additionally, two linear variable differential transformers (LVDTs) were used in order to model the displacement of each end of the tube relative to the collar. All electronic readouts (load cell, cross-head displacement, displacements of the LVDTs, and strains) were recorded on a Strainbook data acquisition system.

*Pull Tests*

The pull tests were performed according to the test program described in [6] in air and at room temperature. The mechanical operation of the MTS system was performed by M. Gallik and

A. Stett, while the electronic recording of the data was done by A. Roslund, all of whom work at Westinghouse's Waltz Mill facility. The sequence of the testing was activation of the Strainbook and confirmation of its recording, initiation of the pull test, continuation of the pull test until approximately two inches of cross-head displacement were achieved, and finally, the cessation of pull testing and electronic recording of data.

*Post-Test Evaluations*

After the pull testing was complete, another set of eddy current measurements were made at Westinghouse's Waltz Mill facility by R. Pocratsky. Again, both the 3-coil +point and standard bobbin coil probes were used.

*Monte Carlo Analysis*

In support of the test program, Monte Carlo simulations were run, based on means and standard deviations from the test data, in order to determine a 5/50 bound on pull force. The simulations were performed in two ways and on a tube OD basis: one simulation considered the thirteen inch expansions only, and the other simulation considered all nine tests together, ignoring expansion length difference. Seven distributions were chosen and the fitting parameters set so that the resulting distribution has the mean and standard deviation of the test data. The first was a truncated normal distribution. The other six were chosen so that their domains span zero to positive infinity, their domains are continuous, and fitting parameters are within their allowable ranges. They were lognormal, Erlang, Gamma, inverse Gaussian, Pearson Type V, and Weibull. In each simulation, 100,000 iterations were run.

**Discussion of Key Parameters**

Tube pull out force capacity (based on residual contact pressure) can be derived from the measured pull out forces from the test that simulate the as-manufactured condition of the steam generators. All of the tests performed to date have demonstrated that a positive value of residual contact pressure exists after the hydraulic expansion process. However, the results from these tests depend on a number of factors including dimensional variations of the tubes and tube collars, surface finish variations, potential manufacturing artifacts on the tubesheet (collar) bore, tube joint process variables, and material properties of the test specimens. The key items identified are addressed below.

The NRC staff has raised the concern that sufficient information must be provided to adequately characterize the potential range in values of residual contact pressure between the tube and the tubesheet (due to the hydraulic expansion process) which may be encountered within the whole plant [7]. At that time, only limited pull out data existed upon which the residual contact pressure was estimated. The staff pointed out [7] that the residual contact pressure, and thus the residual load capacity, is highly sensitive to several parameters including hydraulic expansion pressure, tube yield strength, tube material strain hardening properties, and initial (pre-expansion) gap between the tube and the tubesheet. The NRC staff further pointed out in [7] that additional information was necessary to establish whether the pull out test specimens

adequately envelop the range of values of those parameters that may be encountered in the as-built steam generators.

Consequently, two actions have been taken to address the NRC staff concerns. First, an analysis was performed to identify the key parameters that affect the residual contact pressure and to quantify the effects of uncertainties. Secondly, a new pull out test program was initiated to provide test results that can be directly compared to the key parameters as identified by analysis in support of the development of the H* criterion.

The analysis model used to evaluate the residual contact pressure was a two-dimensional, plane strain, finite element model using the ANSYS computer code as described in Section 7 of [8]. Based on a review of Table 7-3 of [8], the key parameters impacting pull out force capacity are:

- Initial tube gap
- Tube yield strength
- Tube joint expansion pressure
- Strain hardening.

Other parameters important to pull out force capacity not considered in the analytical model are surface roughness and variations in the diameter of the tubesheet bore (waviness).

Table 6 provides a comparison of the as-built to as-tested parameters in the new test program. Based on a review of Table 6, several points can be made regarding the key parameters of the pull out testing.

- It is expected that standard gun drilling practices used in the manufacture of steam generators would typically result in nominal gaps between the tube and tubesheet. No special controls were placed on the initial gap size as the test program was meant to be as prototypic as possible.
- The yield strength of the tubes used for the test specimens simulating the as-built configuration of the Model F and Model D5 steam generators was conservatively high compared to the as-built mean values ([ ]$^{a,b,c}$ ksi vs. [ ]$^{a,b,c}$ ksi), because higher yield strengths result in less tube deformation for a given expansion pressure. The yield strength for the tubes used for the Model 44F steam generators was slightly less than the as-built mean yield strength ([ ]$^{a,b,c}$ ksi vs. [ ]$^{a,b,c}$ ksi).
- The expansion pressure used in the manufacture of the test specimen was consistent with what is specified in [3] and is directly applicable to the as-built conditions of the steam generators in the H* fleet.
- The surface roughness of the tubes outer diameters and the collars inner diameters was well within the tolerances of the as-built conditions of the steam generators in the H* fleet.
- The mechanical properties of the materials used for the test specimens are within ASME Code specifications for the respective materials. Thus, use of the ASME Code values for the key parameters of the H* study is valid.

Other differences between the materials used for the test specimens for the pull out tests are addressed below.

The use of mill annealed tube vice thermally treated tubing for the Model F specimens has been evaluated and found to be acceptable. For room temperature testing, the key material property affecting the residual contact pressure is yield strength. The difference between yield strength of mill annealed material and thermally treated material is presented in Table 7 and further discussed below. Based on the similarity of mechanical properties between the two materials, it is concluded that there is no adverse effect on the test results. The yield strength value used for the Model F test specimens was [ ]$^{a,b,c}$ ksi, which would result in a reduction of residual contact pressure [9].

The test specimen collar is manufactured from AISI 1018 cold rolled, carbon steel. The material used in the H* fleet is actually A508 Class 2a carbon steel. The use of the different material does not adversely affect the pull test results since the primary property of the material in this case is elastic flexural rigidity of the tubesheet (i.e., elastic modulus), and since the tube expansion operation does not produce significant yielding of the tubesheet (the yield strength of the AISI 1018 cold rolled, carbon steel at room temperature is ~83 ksi), the use of higher strength material for the collar is acceptable (see pp. 8-9 of [8]). Thus, it is concluded that the pull out testing is representative of the as-built condition of the steam generators in the H* fleet.

**Results**

Table 8 shows the results of the pull tests, while Table 9 through Table 15 shows the results of the Monte Carlo simulations. The latter results are calculated for the pull out force at 0.25 inch displacement.

**Discussion**

Discussion between Westinghouse and the NRC staff has led to the decision that the pull out force of record should be the pull out force at 0.25 inch cross head displacement. The following discussion and analysis will, therefore, be based on that quantity.

Figure 10 plots the pull out force as a function of the collar ID surface roughness. The graph also provides information on the tube expansion lengths and the tube diameters that were tested. Intuitively, it would be expected that tube pull out force would increase with increasing tube diameter (which provides greater surface area in contact), increasing tube expansion length (which does the same thing), and increasing surface roughness. However, the results in Figure 10 do not necessarily support these assumptions. The highest pull out force for 0.25 inch cross head displacement (approximately [ ]$^{a,b,c}$ kips) occurred for both a test specimen with the largest tube OD, the largest collar ID surface roughness, and the smallest expansion length, as well as for a test specimen having the largest tube OD, one of the lowest collar ID surface roughness values, and the smallest expansion length. The next highest pull out force ([ ]$^{a,b,c}$ kips) occurred for tubes with varying degrees of collar ID surface roughness, for all tube ODs, and for all expansion lengths. The lowest pull out force ([ ]$^{a,b,c}$ lbf) occurred for a test

specimen with a 0.75 inch tube OD, a collar ID surface roughness of ~ 50 micro-inch (rms), and an expansion length of 15 inches. The lowest pull out force for a Model F test specimen was less than [ ]$^{a,b,c}$ kips. This specimen had a collar ID surface roughness less than 40 micro-inch (rms) and an expansion length of 13 inches. The lowest pull out force for a Model 44F specimen was less than [ ]$^{a,b,c}$ kips. This specimen had a collar ID surface roughness of less than 40 micro-inch (rms) and a tube expansion length of 15 inches.

Similarly, the pull test results are shown as a function of tube expansion length in Figure 11. These results also show the lack of correlation between pull out force and tube OD and expansion length.

The pull force necessary to move a tube in the collar is a consequence of three main factors: the residual contact pressure due to the hydraulic expansion, the surface roughness of the tube and the collar, and any geometric irregularities due to machining of the tube and collar, which are then subject to hydraulic expansion. As shown by analysis, the initial gap between the outer diameter of the unexpanded tube and the tubesheet bore hole can adversely affect the resulting residual contact pressure. Small variations along the length of the collar ID (waviness) due to the gun drilling process are significant contributors to the pull out resistance. Geometric irregularities are present as initial gaps between the tube and the collar and as bulges in the tubes. One possible explanation for the significant variation in the test results may be that the waviness was not well profiled due to the difficulty of quantifying this variable. Nonetheless, the pull out test results do appear to be consistent with the expected as-built condition.

Recall that nine pull out tests were performed for each tube OD. Analysis of variance (ANOVA in statistics) is a collection of statistical models and their associated procedures in which the observed variance is partitioned into components due to different explanatory variables. In its simplest form, ANOVA provides a statistical test of whether the means of several groups of data are all equal. One such method is called the F-test. Therefore, the F-test was conducted on the pull out test capabilities comparing the variance of each set of 9 samples for each tube diameter using Microsoft EXCEL. The F-test was used to determine whether or not there was any statistical difference between tube OD and pull test results. The answer was that it cannot be concluded that there is any difference in the variance between each sample set and that the means for tube pull out force for each of the outer diameters may be equal. Therefore, it is judged that all of the data can be considered to be one data set.

However, the NRC staff stated in [7] that there is a need to adjust the pull out data so as to produce an estimate of the residual contact pressure that is conservative for the range of H* values that are being proposed. In order to address this concern for the new pull out test data (i.e., the expansion length of some of the pull out test data exceed the calculated H* values), the sample sets for the different tube ODs were not combined. They were separated by expansion length, even though the F-test results suggest that the mean values of the tube pull out capacity are the same for different tube ODs and considering variations in expansion length and surface roughness.

To investigate this further, the Monte Carlo simulations were performed. Each tube OD was broken up into two sets (13 inch expansion length only and all expansion lengths) and

distributions were chosen based on the criteria previously defined. Using the calculated means and standard deviations from each data set, the fitting parameters for the seven distributions chosen were calculated. Note that the fitting parameters for the normal and lognormal distributions are simply the mean and standard deviation. In each case the 5/50 value was recorded, and the lowest of these corresponded to a pull force of [ ]$^{a,c,e}$ lbf. This was calculated for the Model F tube, 13 inch expansion length only, and using the Weibull distribution (see Table 15). This value is very consistent with the lowest actual pull force from the test data ([ ]$^{a,b,c}$ lbf).

**Conclusion**

Based on the results of the pull tests and Monte Carlo analyses, it is concluded that the end cap load used in the H* analysis can be conservatively reduced by [ ]$^{a,c,e}$ lbf. H* can then be recalculated accordingly.

**References**

(1) ASTM E8/E8M-08, "Standard Test Method for Tension Testing of Metallic Materials," West Conshohocken: ASTM International, 2008.

(2) W. B. Middlebrooks, D. L. Harrod, and R. E. Gold, *Nuclear Engineering and Design* 143, 1993, pp. 159-169.

(3) Process Specification 81013RM, "Hydraulic Tube Expansion," Rev.4 through Rev. 10, February 1, 1979 through July 24, 1981.

(4) J. T. Kandra, TP-CDME-08-3, "Test Procedure for Tube Expansion for H*," August 25, 2008.

(5) D. L. Harrod, WNEP-9725, "The Westinghouse Tube-to-Tubesheet Joint Hydraulic Expansion Process," July 1997.

(6) J. T. Kandra, TP-CDME-08-1, "Pull-Out Test Program for H*," August 25, 2008.

(7) NRC Letter, "Wolf Creek Generating Station – Withdrawal of License Amendment on Steam Generator Tube Inspections (TAC No. MD0197)," United States Nuclear Regulatory Commission, Washington, D.C., February 28, 2008.

(8) WCAP-17071-P, "H*: Alternate Repair Criteria for the Tubesheet Expansion Region in Steam Generators with Hydraulically Expanded Tubes (Model F)," April 2009.

(9) DP-SGDA-05-2, "Data Package for H-Star Pull Test of 7/8 Inch Tubing form Simulated Tubesheet, PA-MSC-0199 WOG Program for Steam Generator Models 44F and 51F," November 2005.

(10) LTR-SGMP-09-98, "H* Pull Test Program Summary," Westinghouse Electric Company LLC, July 27, 2009.

**Table 1**
**Chemical Analyses of the A600 Materials Used in This Test Program**

| Steam Generator Model | F | D5 | 44F |
|---|---|---|---|
| Chemical Analysis Source | Plymouth Tube Co. Salisbury, MD | Huntington Alloys, Inc. Huntington, WV | AB Sandvik Steel |
| Heat | NX7368 | 2645 | 752570 |
| Element (w/o) | | | |
| C | 0.04 | 0.033 | 0.025 |
| Mn | 0.41 | 0.34 | 0.79 |
| P | N/A | 0.007 | 0.009 |
| S | 0.001 | 0.001 | 0.002 |
| Si | 0.30 | 0.09 | 0.33 |
| Cr | 14.87 | 15.44 | 16.60 |
| Ni | 76.21 | 75.45 | 72.45 |
| Cu | 0.15 | 0.23 | 0.010 |
| Co | 0.04 | 0.04 | 0.011 |
| Fe | 7.98 | 8.42 | 9.29 |
| B | N/A | 0.003 | N/A |

**Table 2**
**Mechanical Properties of the A600 Materials Used in This Test Program**

| Steam Generator Model | Heat | Mechanical Property Source | $\sigma_Y$ (psi) | $\sigma_{UT}$ (psi) | Elongation (%) |
|---|---|---|---|---|---|
| F | NX7368 | Vendor | 59,700 | 106,600 | 39 |
| | | ITLS | 58,000 | 108,000 | 32 |
| D5 | 2645 | Vendor | 43,000 | 97,000 | 41.5 |
| | | ITLS | 54,000 | 110,000 | 35 |
| 44F | 752570 | Vendor | 47,500 | 101,700 | 45.5 |
| | | ITLS | 46,000 | 101,000 | 40 |

**Table 3**
**Chemical Analyses of the 1018 Cold-Rolled, Carbon Steel Used in This Test Program**

| | | | Element (w/o) | | | | |
|---|---|---|---|---|---|---|---|
| Steel | Chemical Analysis Source | Heat | C | Mn | Si | S | P |
| AISI 1018 | Steel Bar Corp. Greensboro, NC | 777553 | 0.17 | 0.84 | 0.27 | 0.030 | 0.005 |
| AISI 1018 | Steel Bar Corp. Greensboro, NC | 730492 | 0.18 | 0.79 | 0.22 | 0.030 | 0.010 |

**Table 4**
**Mechanical Properties of the 1018 Cold-Rolled, Carbon Steel Used in This Test Program**

| Steel | Heat | Mechanical Property Source | $\sigma_Y$ (ksi) | $\sigma_{UT}$ (ksi) | Elongation (%) |
|---|---|---|---|---|---|
| AISI 1018 | 777553 | DuBose National Energy Services, Inc. Clinton, NC | 83.0 | 90.0 | 18 |
| AISI 1018 | 730492 | DuBose National Energy Services, Inc. Clinton, NC | 67.5 | 79.3 | 25 |

**Table 5**
**Steam Generator Tube and Collar Pairings Used in This Test Program**

| Tube | Heat | Collar | Heat |
|---|---|---|---|
| 17-688-01A | NX7368 | 15-699-01A | 777553 |
| 17-688-02A | NX7368 | 15-699-02A | 777553 |
| 17-688-03 | NX7368 | 15-699-03A | 777553 |
| 19-688-01 | NX7368 | 17-699-01A | 777553 |
| 19-688-02 | NX7368 | 17-699-02A | 777553 |
| 19-688-03 | NX7368 | 17-699-03A | 777553 |
| 21-688-01 | NX7368 | 19-699-01A | 777553 |
| 21-688-02 | NX7368 | 19-699-02A | 777553 |
| 21-688-03 | NX7368 | 19-699-03A | 777553 |
| 17-750-01A | 2645 | 15-762-01A | 777553 |
| 17-750-02A | 2645 | 15-762-02A | 777553 |
| 17-750-03 | 2645 | 15-699-03 | 730492 |
| 19-750-01 | 2645 | 17-762-01A | 777553 |
| 19-750-02 | 2645 | 17-762-02A | 777553 |
| 19-750-03 | 2645 | 17-762-03A | 777553 |
| 21-750-01 | 2645 | 19-762-01A | 777553 |
| 21-750-02 | 2645 | 19-762-02A | 777553 |
| 21-750-03 | 2645 | 19-762-03A | 777553 |
| 17-875-01A | 752570 | 15-888-01A | 777553 |
| 17-875-02A | 752570 | 15-888-02A | 777553 |
| 17-875-03 | 752570 | 15-762-03 | 730492 |
| 19-875-01 | 752570 | 17-888-01A | 777553 |
| 19-875-02 | 752570 | 17-888-02A | 777553 |
| 19-875-03 | 752570 | 17-888-03A | 777553 |
| 21-875-01 | 752570 | 19-888-01A | 777553 |
| 21-875-02 | 752570 | 19-888-02A | 777553 |
| 21-875-03 | 752570 | 19-888-03A | 777553 |

**Table 6**
**Residual Contact Pressure Critical Parameter Comparison**

| Key Parameters | Model F | | Model D5 | | Models 44F -51F | |
|---|---|---|---|---|---|---|
| | As-Built | As-Tested | As-Built | As-Tested | As-Built | As-Tested |
| Average Initial Gap (inches) | | | | | | |
| Tube Yield Strength (ksi) | | | | | | |
| Expansion Pressure (ksi) | | | | | | |
| Tube Outer Diameter Surface Roughness μ in. rms | | | | | | |
| Collar Inner Diameter Surface Roughness μ in. rms | | | | | | |
| Tube OD (in) | | | | | | |
| Collar ID (in) | | | | | | |

a,c,e

**Table 7**
**Comparison of Yield Strength Between Mill Annealed and Thermally Treated Alloy 600**

| | Alloy 600 Mill Annealed As-Tested | Alloy 600 Thermally Treated As-Built |
|---|---|---|
| Minimum | | |
| Mean | | |
| Maximum | | |
| Standard Deviation | | |
| Number of Tests | 361 | 307 |
| Tube Size (OD) | 7/8 inch | 7/8 inch |
| Data | Reference [1] | Reference [1] |
| Yield Strength values are in units of ksi. | | |

a,c,e

**Table 8**
**Results of the Pull Testing**

| Tube ID | Heat | Collar ID | Heat | Load at 0.25" Displacement (kip) | Max. Load (kip) | Displacement at Max. Load (in) |
|---|---|---|---|---|---|---|
| 17-688-01A | NX7368 | 15-699-01A | 777553 | | | |
| 17-688-02A | NX7368 | 15-699-02A | 777553 | | | |
| 17-688-03 | NX7368 | 15-699-03A | 777553 | | | |
| 19-688-01 | NX7368 | 17-699-01A | 777553 | | | |
| 19-688-02 | NX7368 | 17-699-02A | 777553 | | | |
| 19-688-03 | NX7368 | 17-699-03A | 777553 | | | |
| 21-688-01 | NX7368 | 19-699-01A | 777553 | | | |
| 21-688-02 | NX7368 | 19-699-02A | 777553 | | | |
| 21-688-03 | NX7368 | 19-699-03A | 777553 | | | |
| 17-750-01A | 2645 | 15-762-01A | 777553 | | | |
| 17-750-02A | 2645 | 15-762-02A | 777553 | | | |
| 17-750-03 | 2645 | 15-699-03 | 730492 | | | |
| 19-750-01 | 2645 | 17-762-01A | 777553 | | | |
| 19-750-02 | 2645 | 17-762-02A | 777553 | | | |
| 19-750-03 | 2645 | 17-762-03A | 777553 | | | |
| 21-750-01 | 2645 | 19-762-01A | 777553 | | | |
| 21-750-02 | 2645 | 19-762-02A | 777553 | | | |
| 21-750-03 | 2645 | 19-762-03A | 777553 | | | |
| 17-875-01A | 752570 | 15-888-01A | 777553 | | | |
| 17-875-02A | 752570 | 15-888-02A | 777553 | | | |
| 17-875-03 | 752570 | 15-762-03 | 730492 | | | |
| 19-875-01 | 752570 | 17-888-01A | 777553 | | | |
| 19-875-02 | 752570 | 17-888-02A | 777553 | | | |
| 19-875-03 | 752570 | 17-888-03A | 777553 | | | |
| 21-875-01 | 752570 | 19-888-01A | 777553 | | | |
| 21-875-02 | 752570 | 19-888-02A | 777553 | | | |
| 21-875-03 | 752570 | 19-888-03A | 777553 | | | |

a,b,c

**Table 9**
**Monte Carlo Results for the Truncated Normal Distribution**

| Distribution | Normal Distribution (truncated at 0) | | | |
|---|---|---|---|---|
| Case 1 | Parameters to Define the Distribution | | | 5/50 Pull Out Force (kip) |
| Model F 13" Expansion | Name | Mean | Stand. Dev. | [ ]a,c,e |
| | Symbol | μ | σ | |
| | Value | [ ]a,c,e | [ ]a,c,e | |
| Case 2 | Parameters to Define the Distribution | | | 5/50 Pull Out Force (kip) |
| Model F All Expansions | Name | Mean | Stand. Dev. | [ ]a,c,e |
| | Symbol | μ | σ | |
| | Value | [ ]a,c,e | [ ]a,c,e | |
| Case 3 | Parameters to Define the Distribution | | | 5/50 Pull Out Force (kip) |
| Model D5 13" Expansion | Name | Mean | Stand. Dev. | [ ]a,c,e |
| | Symbol | μ | σ | |
| | Value | [ ]a,c,e | [ ]a,c,e | |
| Case 4 | Parameters to Define the Distribution | | | 5/50 Pull Out Force (kip) |
| Model D5 All Expansions | Name | Mean | Stand. Dev. | [ ]a,c,e |
| | Symbol | μ | σ | |
| | Value | [ ]a,c,e | [ ]a,c,e | |
| Case 5 | Parameters to Define the Distribution | | | 5/50 Pull Out Force (kip) |
| Model 44F 13" Expansion | Name | Mean | Stand. Dev. | [ ]a,c,e |
| | Symbol | μ | σ | |
| | Value | [ ]a,c,e | [ ]a,c,e | |
| Case 6 | Parameters to Define the Distribution | | | 5/50 Pull Out Force (kip) |
| Model 44F All Expansions | Name | Mean | Stand. Dev. | [ ]a,c,e |
| | Symbol | μ | σ | |
| | Value | [ ]a,c,e | [ ]a,c,e | |

**Table 10**
**Monte Carlo Results for the LogNormal Distribution**

| Distribution | Lognormal Distribution | | | |
|---|---|---|---|---|
| Case 1 | Parameters to Define the Distribution | | | 5/50 Pull Out Force (kip) |
| Model F 13" Expansion | Name | Mean | Stand. Dev. | [ ]a,c,e |
| | Symbol | μ | σ | |
| | Value | [ ]a,c,e | [ ]a,c,e | |
| Case 2 | Parameters to Define the Distribution | | | 5/50 Pull Out Force (kip) |
| Model F All Expansions | Name | Mean | Stand. Dev. | [ ]a,c,e |
| | Symbol | μ | σ | |
| | Value | [ a,c,e | [ ]a,c,e | |
| Case 3 | Parameters to Define the Distribution | | | 5/50 Pull Out Force (kip) |
| Model D5 13" Expansion | Name | Mean | Stand. Dev. | [ ]a,c,e |
| | Symbol | μ | σ | |
| | Value | [ ]a,c,e | [ ]a,c,e | |
| Case 4 | Parameters to Define the Distribution | | | 5/50 Pull Out Force (kip) |
| Model D5 All Expansions | Name | Mean | Stand. Dev. | [ ]a,c,e |
| | Symbol | μ | σ | |
| | Value | [ ]a,c,e | [ ]a,c,e | |
| Case 5 | Parameters to Define the Distribution | | | 5/50 Pull Out Force (kip) |
| Model 44F 13" Expansion | Name | Mean | Stand. Dev. | [ ]a,c,e |
| | Symbol | μ | σ | |
| | Value | [ ]a,c,e | [ ]a,c,e | |
| Case 6 | Parameters to Define the Distribution | | | 5/50 Pull Out Force (kip) |
| Model 44F All Expansions | Name | Mean | Stand. Dev. | [ ]a,c,e |
| | Symbol | μ | σ | |
| | Value | [ ]a,c,e | [ ]a,c,e | |

**Table 11**
**Monte Carlo Results for the Erlang Distribution**

| Distribution | Erlang Distribution | | | |
|---|---|---|---|---|
| Case 1 | Parameters to Define the Distribution | | | 5/50 Pull Out Force (kip) |
| Model F 13" Expansion | Name | Cont. Shape Par. | Cont. Scale Par. | [ ]a,c,e |
| | Symbol | m | β | |
| | Value | [ ]a,c,e | [ ]a,c,e | |
| Case 2 | Parameters to Define the Distribution | | | 5/50 Pull Out Force (kip) |
| Model F All Expansions | Name | Cont. Shape Par. | Cont. Scale Par. | [ ]a,c,e |
| | Symbol | m | β | |
| | Value | [ ]a,c,e | [ ]a,c,e | |
| Case 3 | Parameters to Define the Distribution | | | 5/50 Pull Out Force (kip) |
| Model D5 13" Expansion | Name | Cont. Shape Par. | Cont. Scale Par. | [ ]a,c,e |
| | Symbol | m | β | |
| | Value | [ ]a,c,e | [ ]a,c,e | |
| Case 4 | Parameters to Define the Distribution | | | 5/50 Pull Out Force (kip) |
| Model D5 All Expansions | Name | Cont. Shape Par. | Cont. Scale Par. | [ ]a,c,e |
| | Symbol | m | β | |
| | Value | [ ]a,c,e | [ ]a,c,e | |
| Case 5 | Parameters to Define the Distribution | | | 5/50 Pull Out Force (kip) |
| Model 44F 13" Expansion | Name | Cont. Shape Par. | Cont. Scale Par. | [ ]a,c,e |
| | Symbol | m | β | |
| | Value | [ ]a,c,e | [ ]a,c,e | |
| Case 6 | Parameters to Define the Distribution | | | 5/50 Pull Out Force (kip) |
| Model 44F All Expansions | Name | Cont. Shape Par. | Cont. Scale Par. | [ ]a,c,e |
| | Symbol | m | β | |
| | Value | [ ]a,c,e | [ ]a,c,e | |

**Table 12**
**Monte Carlo Results for the Gamma Distribution**

| Distribution | Gamma Distribution | | | |
|---|---|---|---|---|
| Case 1 | Parameters to Define the Distribution | | | 5/50 Pull Out Force (kip) |
| Model F 13" Expansion | Name | Cont. Shape Par. | Cont. Scale Par. | [ ]a,c,e |
| | Symbol | α | β | |
| | Value | [ ]a,c,e | [ ]a,c,e | |
| Case 2 | Parameters to Define the Distribution | | | 5/50 Pull Out Force (kip) |
| Model F All Expansions | Name | Cont. Shape Par. | Cont. Scale Par. | [ ]a,c,e |
| | Symbol | α | β | |
| | Value | [ ]a,c,e | [ ]a,c,e | |
| Case 3 | Parameters to Define the Distribution | | | 5/50 Pull Out Force (kip) |
| Model D5 13" Expansion | Name | Cont. Shape Par. | Cont. Scale Par. | [ ]a,c,e |
| | Symbol | α | β | |
| | Value | [ ]a,c,e | [ ]a,c,e | |
| Case 4 | Parameters to Define the Distribution | | | 5/50 Pull Out Force (kip) |
| Model D5 All Expansions | Name | Cont. Shape Par. | Cont. Scale Par. | [ ]a,c,e |
| | Symbol | α | β | |
| | Value | [ ]a,c,e | [ ]a,c,e | |
| Case 5 | Parameters to Define the Distribution | | | 5/50 Pull Out Force (kip) |
| Model 44F 13" Expansion | Name | Cont. Shape Par. | Cont. Scale Par. | [ ]a,c,e |
| | Symbol | α | β | |
| | Value | [ ]a,c,e | [ ]a,c,e | |
| Case 6 | Parameters to Define the Distribution | | | 5/50 Pull Out Force (kip) |
| Model 44F All Expansions | Name | Cont. Shape Par. | Cont. Scale Par. | [ ]a,c,e |
| | Symbol | α | β | |
| | Value | [ ]a,c,e | [ ]a,c,e | |

**Table 13**
**Monte Carlo Results for the Inverse Gaussian Distribution**

| Distribution | Inverse Gaussian Distribution | | | |
|---|---|---|---|---|
| Case 1 | Parameters to Define the Distribution | | | 5/50 Pull Out Force (kip) |
| Model F 13" Expansion | Name | Cont. Par. | Cont. Par. | [ ]a,c,e |
| | Symbol | μ | λ | |
| | Value | [ ]a,c,e | [ ]a,c,e | |
| Case 2 | Parameters to Define the Distribution | | | 5/50 Pull Out Force (kip) |
| Model F All Expansions | Name | Cont. Par. | Cont. Par. | [ ]a,c,e |
| | Symbol | μ | λ | |
| | Value | [ ]a,c,e | [ ]a,c,e | |
| Case 3 | Parameters to Define the Distribution | | | 5/50 Pull Out Force (kip) |
| Model D5 13" Expansion | Name | Cont. Par. | Cont. Par. | [ ]a,c,e |
| | Symbol | μ | λ | |
| | Value | [ ]a,c,e | [ ]a,c,e | |
| Case 4 | Parameters to Define the Distribution | | | 5/50 Pull Out Force (kip) |
| Model D5 All Expansions | Name | Cont. Par. | Cont. Par. | [ ]a,c,e |
| | Symbol | μ | λ | |
| | Value | [ ]a,c,e | [ ]a,c,e | |
| Case 5 | Parameters to Define the Distribution | | | 5/50 Pull Out Force (kip) |
| Model 44F 13" Expansion | Name | Cont. Par. | Cont. Par. | [ ]a,c,e |
| | Symbol | μ | λ | |
| | Value | [ ]a,c,e | [ ]a,c,e | |
| Case 6 | Parameters to Define the Distribution | | | 5/50 Pull Out Force (kip) |
| Model 44F All Expansions | Name | Cont. Par. | Cont. Par. | [ ]a,c,e |
| | Symbol | μ | λ | |
| | Value | [ ]a,c,e | [ ]a,c,e | |

**Table 14**
**Monte Carlo Results for the Pearson Type V Distribution**

| Distribution | Pearson Type V Distribution | | | |
|---|---|---|---|---|
| Case 1 | Parameters to Define the Distribution | | | 5/50 Pull Out Force (kip) |
| Model F 13" Expansion | Name | Cont. Shape Par. | Cont. Scale Par. | [ ]a,c,e |
| | Symbol | α | β | |
| | Value | [ ]a,c,e | [ ]a,c,e | |
| Case 2 | Parameters to Define the Distribution | | | 5/50 Pull Out Force (kip) |
| Model F All Expansions | Name | Cont. Shape Par. | Cont. Scale Par. | [ ]a,c,e |
| | Symbol | α | β | |
| | Value | [ ]a,c,e | [ ]a,c,e | |
| Case 3 | Parameters to Define the Distribution | | | 5/50 Pull Out Force (kip) |
| Model D5 13" Expansion | Name | Cont. Shape Par. | Cont. Scale Par. | [ ]a,c,e |
| | Symbol | α | β | |
| | Value | [ ]a,c,e | [ ]a,c,e | |
| Case 4 | Parameters to Define the Distribution | | | 5/50 Pull Out Force (kip) |
| Model D5 All Expansions | Name | Cont. Shape Par. | Cont. Scale Par. | [ ]a,c,e |
| | Symbol | α | β | |
| | Value | [ ]a,c,e | [ ]a,c,e | |
| Case 5 | Parameters to Define the Distribution | | | 5/50 Pull Out Force (kip) |
| Model 44F 13" Expansion | Name | Cont. Shape Par. | Cont. Scale Par. | [ ]a,c,e |
| | Symbol | α | β | |
| | Value | [ ]a,c,e | [ ]a,c,e | |
| Case 6 | Parameters to Define the Distribution | | | 5/50 Pull Out Force (kip) |
| Model 44F All Expansions | Name | Cont. Shape Par. | Cont. Scale Par. | [ ]a,c,e |
| | Symbol | α | β | |
| | Value | [ ]a,c,e | [ ]a,c,e | |

**Table 15**
**Monte Carlo Results for the Weibull Distribution**

| Distribution | Weibull Distribution | | | |
|---|---|---|---|---|
| Case 1 | Parameters to Define the Distribution | | | 5/50 Pull Out Force (kip) |
| Model F 13" Expansion | Name | Cont. Shape Par. | Cont. Scale Par. | [ ]a,c,e |
| | Symbol | α | β | |
| | Value | [ ]a,c,e | [ ]a,c,e | |
| Case 2 | Parameters to Define the Distribution | | | 5/50 Pull Out Force (kip) |
| Model F All Expansions | Name | Cont. Shape Par. | Cont. Scale Par. | [ ]a,c,e |
| | Symbol | α | β | |
| | Value | [ ]a,c,e | [ ]a,c,e | |
| Case 3 | Parameters to Define the Distribution | | | 5/50 Pull Out Force (kip) |
| Model D5 13" Expansion | Name | Cont. Shape Par. | Cont. Scale Par. | [ ]a,c,e |
| | Symbol | α | β | |
| | Value | [ ]a,c,e | [ ]a,c,e | |
| Case 4 | Parameters to Define the Distribution | | | 5/50 Pull Out Force (kip) |
| Model D5 All Expansions | Name | Cont. Shape Par. | Cont. Scale Par. | [ ]a,c,e |
| | Symbol | α | β | |
| | Value | [ ]a,c,e | [ ]a,c,e | |
| Case 5 | Parameters to Define the Distribution | | | 5/50 Pull Out Force (kip) |
| Model 44F 13" Expansion | Name | Cont. Shape Par. | Cont. Scale Par. | [ ]a,c,e |
| | Symbol | α | β | |
| | Value | [ ]a,c,e | [ ]a,c,e | |
| Case 6 | Parameters to Define the Distribution | | | 5/50 Pull Out Force (kip) |
| Model 44F All Expansions | Name | Cont. Shape Par. | Cont. Scale Par. | [ ]a,c,e |
| | Symbol | α | β | |
| | Value | [ ]a,c,e | [ ]a,c,e | |

**Figure 1**
**The Model F 13 Inch Expansion Tube/Collar Assembly**

a,c,e

[ ]

**Figure 2**
**The Model F 15 Inch Expansion Tube/Collar Assembly**

a,c,e

[ ]

**Figure 3**
**The Model F 17 Inch Expansion Tube/Collar Assembly**

a,c,e

[ ]

**Figure 4**
**The Model D5 13 Inch Expansion Tube/Collar Assembly**

a,c,e

[ ]

**Figure 5**
**The Model D5 15 Inch Expansion Tube/Collar Assembly**

a,c,e

**Figure 6**
**The Model D5 17 Inch Expansion Tube/Collar Assembly**

a,c,e

[ ]

**Figure 7**
**The Model 44F 13 Inch Expansion Tube/Collar Assembly**

a,c,e

**Figure 8**
**The Model 44F 15 Inch Expansion Tube/Collar Assembly**

a,c,e

**Figure 9**
**The Model 44F 17 Inch Expansion Tube/Collar Assembly**

a,c,e

[ ]

**Figure 10**
**A Plot of Pull Out Force vs. Surface Roughness**

a,c,e

[ ]

**Figure 11**
**The Pull Out Force vs. Expansion Length for a Given Tube OD**

a,c,e

[ ]

ATTACHMENT 12

Catawba Unit 2 Site Specific Response to (Industry) NRC RAI Questions 21, 22, and 23

Reference 1 (below) provided a request for additional information to Southern Nuclear Operating Company related to their application for a permanent alternate repair criterion based on WCAP-17071-P, Revision 0. Since Reference 1 is applicable to the Duke application, a response is being provided by Duke.

Provided below are response to questions 21, 22, and 23. The specific NRC questions are provided in italics.

*21. The limiting leakage factor for VEGP is greater than 2.0 per Reference 2. The reporting requirement proposed by VEGP only requires them to report if they use a leakage factor of less than 2.0. The NRC staff understands that the licensee does not want to give a false impression that it can measure very small leak rates; however, the NRC staff feels it is appropriate for the licensee to use a number that bounds the plant-specific limiting leakage factor in Reference 2.*

*Please discuss your plans to incorporate a limiting leakage factor that bounds the value in Reference 1.*

**Response:** As discussed in Attachment 1, Duke will use the plant specific leakage factor of 3.27 based on Table 9-7 of WCAP-17072-P, as revised by the response to RAI 24 and as increased per Attachment 16.

*22. In the May 19, 2009, letter, VEGP commits to monitor for tube slippage as part of the SG tube inspection program. The "due date/event" is prior to the start of Refueling Outage 1R15. It is not clear whether the planned monitoring will be performed once and whether it only applies to Unit 1. The commitment should be modified to indicate that the tube slippage will be monitored at both units during every SG tube inspection outage.*

**Response:** Tube slippage monitoring is only applicable to Catawba Unit 2. Duke commits to monitor for tube slippage as part of the Catawba Unit 2 steam generator tube inspection program.

*23. In the May 19, 2009, letter, VEGP commits to determine the position of the bottom of the expansion transition in relation to the top of the tubesheet and to enter "any significant deviation" into their corrective action program. This is a one-time verification prior to implementation of H*. The commitment should be modified to also include a commitment to notify the NRC staff if significant deviations in the location of the bottom of the expansion transition relative to the top of the tubesheet are detected.*

**Response:** Duke commits to perform a one-time verification of the tube expansion to locate any significant deviations in the distance from the top of the tubesheet to the bottom of the expansion transition (BET). If any deviations are found, the condition will be entered into the corrective action program and

dispositioned. Additionally, Duke commits to notify the NRC of significant deviations.

**References:**

1) Letter dated July 10, 2009, from D. Wright, USNRC, to M.J. Ajluni, Southern Nuclear Operating Company, Inc., "Vogtle Electric Generating Plant, Units 1 and 2, Request for Additional Information Regarding Steam Generator Program (TAC NOS. ME1339 and ME1340)"

2) WCAP-17071-P, Revision 0, "H*: Alternate Repair Criteria for the Tubesheet Expansion Region in Steam Generators with Hydraulically Expanded Tubes (Model F)", April 2009

ATTACHMENT 13

Westinghouse Authorization Letter CAW-09-2664 with Accompanying Affidavit, Proprietary Information Notice, and Copyright Notice (LTR-SGMP-09-109 P-Attachment)

Westinghouse

Westinghouse Electric Company
Nuclear Services
P.O. Box 355
Pittsburgh, Pennsylvania 15230-0355
USA

U.S. Nuclear Regulatory Commission
Document Control Desk
Washington, DC 20555-0001

Direct tel: (412) 374-4643
Direct fax: (412) 374-3846
e-mail: greshaja@westinghouse.com

Our ref: CAW-09-2664

August 27, 2009

APPLICATION FOR WITHHOLDING PROPRIETARY
INFORMATION FROM PUBLIC DISCLOSURE

Subject: LTR-SGMP-09-109 P-Attachment, "Response to NRC Request for Additional Information on H*; RAI # 4; Model F and Model D5 Steam Generators," dated August 2009 (Proprietary)

The proprietary information for which withholding is being requested in the above-referenced report is further identified in Affidavit CAW-09-2664 signed by the owner of the proprietary information, Westinghouse Electric Company LLC. The affidavit, which accompanies this letter, sets forth the basis on which the information may be withheld from public disclosure by the Commission and addresses with specificity the considerations listed in paragraph (b)(4) of 10 CFR Section 2.390 of the Commission's regulations.

Accordingly, this letter authorizes the utilization of the accompanying affidavit by Duke Energy.

Correspondence with respect to the proprietary aspects of the application for withholding or the Westinghouse affidavit should reference this letter, CAW-09-2664, and should be addressed to J. A. Gresham, Manager, Regulatory Compliance and Plant Licensing, Westinghouse Electric Company LLC, P.O. Box 355, Pittsburgh, Pennsylvania 15230-0355.

Very truly yours,

J.A. Gresham, Manager
Regulatory Compliance and Plant Licensing

Enclosures

cc: G. Bacuta, (NRC OWFN 12E-1)

bcc: J. A. Gresham (ECE 4-7A) 1L
R. Bastien, 1L (Nivelles, Belgium)
C. Brinkman, 1L (Westinghouse Electric Co., 12300 Twinbrook Parkway, Suite 330, Rockville, MD 20852)
RCPL Administrative Aide (ECE 4-7A) 1L (letter and affidavit only)
G. W. Whiteman, Waltz Mill
H. O. Lagally, Waltz Mill
C. D. Cassino, Waltz Mill
J. T. Kandra, Waltz Mill
D. C. Beddingfield, ECE 558B

CAW-09-2664

# AFFIDAVIT

COMMONWEALTH OF PENNSYLVANIA:

ss

COUNTY OF ALLEGHENY:

Before me, the undersigned authority, personally appeared J. A. Gresham, who, being by me duly sworn according to law, deposes and says that he is authorized to execute this Affidavit on behalf of Westinghouse Electric Company LLC (Westinghouse), and that the averments of fact set forth in this Affidavit are true and correct to the best of his knowledge, information, and belief:

J. A. Gresham, Manager
Regulatory Compliance and Plant Licensing

Sworn to and subscribed before me
this 27th day of August, 2009

Sharon L. Markle
Notary Public

COMMONWEALTH OF PENNSYLVANIA
Notarial Seal
Sharon L. Markle, Notary Public
Monroeville Boro, Allegheny County
My Commission Expires Jan. 29, 2011
Member, Pennsylvania Association of Notaries

(1) I am Manager, Regulatory Compliance and Plant Licensing, in Nuclear Services, Westinghouse Electric Company LLC (Westinghouse), and as such, I have been specifically delegated the function of reviewing the proprietary information sought to be withheld from public disclosure in connection with nuclear power plant licensing and rule making proceedings, and am authorized to apply for its withholding on behalf of Westinghouse.

(2) I am making this Affidavit in conformance with the provisions of 10 CFR Section 2.390 of the Commission's regulations and in conjunction with the Westinghouse "Application for Withholding" accompanying this Affidavit.

(3) I have personal knowledge of the criteria and procedures utilized by Westinghouse in designating information as a trade secret, privileged or as confidential commercial or financial information.

(4) Pursuant to the provisions of paragraph (b)(4) of Section 2.390 of the Commission's regulations, the following is furnished for consideration by the Commission in determining whether the information sought to be withheld from public disclosure should be withheld.

(i) The information sought to be withheld from public disclosure is owned and has been held in confidence by Westinghouse.

(ii) The information is of a type customarily held in confidence by Westinghouse and not customarily disclosed to the public. Westinghouse has a rational basis for determining the types of information customarily held in confidence by it and, in that connection, utilizes a system to determine when and whether to hold certain types of information in confidence. The application of that system and the substance of that system constitute Westinghouse policy and provide the rational basis required.

Under that system, information is held in confidence if it falls in one or more of several types, the release of which might result in the loss of an existing or potential competitive advantage, as follows:

(a) The information reveals the distinguishing aspects of a process (or component, structure, tool, method, etc.) where prevention of its use by any of

Westinghouse's competitors without license from Westinghouse constitutes a competitive economic advantage over other companies.

(b) It consists of supporting data, including test data, relative to a process (or component, structure, tool, method, etc.), the application of which data secures a competitive economic advantage, e.g., by optimization or improved marketability.

(c) Its use by a competitor would reduce his expenditure of resources or improve his competitive position in the design, manufacture, shipment, installation, assurance of quality, or licensing a similar product.

(d) It reveals cost or price information, production capacities, budget levels, or commercial strategies of Westinghouse, its customers or suppliers.

(e) It reveals aspects of past, present, or future Westinghouse or customer funded development plans and programs of potential commercial value to Westinghouse.

(f) It contains patentable ideas, for which patent protection may be desirable.

There are sound policy reasons behind the Westinghouse system which include the following:

(a) The use of such information by Westinghouse gives Westinghouse a competitive advantage over its competitors. It is, therefore, withheld from disclosure to protect the Westinghouse competitive position.

(b) It is information that is marketable in many ways. The extent to which such information is available to competitors diminishes the Westinghouse ability to sell products and services involving the use of the information.

(c) Use by our competitor would put Westinghouse at a competitive disadvantage by reducing his expenditure of resources at our expense.

(d) Each component of proprietary information pertinent to a particular competitive advantage is potentially as valuable as the total competitive advantage. If competitors acquire components of proprietary information, any one component may be the key to the entire puzzle, thereby depriving Westinghouse of a competitive advantage.

(e) Unrestricted disclosure would jeopardize the position of prominence of Westinghouse in the world market, and thereby give a market advantage to the competition of those countries.

(f) The Westinghouse capacity to invest corporate assets in research and development depends upon the success in obtaining and maintaining a competitive advantage.

(iii) The information is being transmitted to the Commission in confidence and, under the provisions of 10 CFR Section 2.390, it is to be received in confidence by the Commission.

(iv) The information sought to be protected is not available in public sources or available information has not been previously employed in the same original manner or method to the best of our knowledge and belief.

(v) The proprietary information sought to be withheld in this submittal is that which is appropriately marked in LTR-SGMP-09-109 P-Attachment, "Response to NRC Request for Additional Information on H*; RAI # 4; Model F and Model D5 Steam Generators," dated August 2009 (Proprietary), for submittal to the Commission, being transmitted by Duke Energy letter and Application for Withholding Proprietary Information from Public Disclosure to the Document Control Desk. The proprietary information as submitted for use by Westinghouse for Catawba Unit 2 is expected to be applicable to other licensee submittals in support of implementing an alternate repair criterion, called H*, that does not require an eddy current inspection and plugging of steam generator tubes below a certain distance from the top of the tubesheet.

This information is part of that which will enable Westinghouse to:

(a) Provide documentation of the analyses, methods, and testing which support the implementation of an alternate repair criterion, designated as H*, for a portion of the tubes within the tubesheet of the Catawba Unit 2 steam generators.

(b) Assist the customer in obtaining NRC approval of the Technical Specification changes associated with the alternate repair criterion.

Further this information has substantial commercial value as follows:

(a) Westinghouse plans to sell the use of similar information to its customers for the purposes of meeting NRC requirements for licensing documentation.

(b) Westinghouse can sell support and defense of the technology to its customers in the licensing process.

Public disclosure of this proprietary information is likely to cause substantial harm to the competitive position of Westinghouse because it would enhance the ability of competitors to provide similar calculation, evaluation and licensing defense services for commercial power reactors without commensurate expenses. Also, public disclosure of the information would enable others to use the information to meet NRC requirements for licensing documentation without purchasing the right to use the information.

The development of the technology described in part by the information is the result of applying the results of many years of experience in an intensive Westinghouse effort and the expenditure of a considerable sum of money.

In order for competitors of Westinghouse to duplicate this information, similar technical programs would have to be performed and a significant manpower effort, having the requisite talent and experience, would have to be expended.

Further the deponent sayeth not.

## PROPRIETARY INFORMATION NOTICE

Transmitted herewith are proprietary and/or non-proprietary versions of documents furnished to the NRC in connection with requests for generic and/or plant-specific review and approval.

In order to conform to the requirements of 10 CFR 2.390 of the Commission's regulations concerning the protection of proprietary information so submitted to the NRC, the information which is proprietary in the proprietary versions is contained within brackets, and where the proprietary information has been deleted in the non-proprietary versions, only the brackets remain (the information that was contained within the brackets in the proprietary versions having been deleted). The justification for claiming the information so designated as proprietary is indicated in both versions by means of lower case letters (a) through (f) located as a superscript immediately following the brackets enclosing each item of information being identified as proprietary or in the margin opposite such information. These lower case letters refer to the types of information Westinghouse customarily holds in confidence identified in Sections (4)(ii)(a) through (4)(ii)(f) of the affidavit accompanying this transmittal pursuant to 10 CFR 2.390(b)(1).

## COPYRIGHT NOTICE

The reports transmitted herewith each bear a Westinghouse copyright notice. The NRC is permitted to make the number of copies of the information contained in these reports which are necessary for its internal use in connection with generic and plant-specific reviews and approvals as well as the issuance, denial, amendment, transfer, renewal, modification, suspension, revocation, or violation of a license, permit, order, or regulation subject to the requirements of 10 CFR 2.390 regarding restrictions on public disclosure to the extent such information has been identified as proprietary by Westinghouse, copyright protection notwithstanding. With respect to the non-proprietary versions of these reports, the NRC is permitted to make the number of copies beyond those necessary for its internal use which are necessary in order to have one copy available for public viewing in the appropriate docket files in the public document room in Washington, DC and in local public document rooms as may be required by NRC regulations if the number of copies submitted is insufficient for this purpose. Copies made by the NRC must include the copyright notice in all instances and the proprietary notice if the original was identified as proprietary.

Duke Energy
Letter for Transmittal to the NRC

The following paragraphs should be included in your letter to the NRC:

Enclosed are:

1. 1 copy of LTR-SGMP-09-109 P-Attachment, "Response to NRC Request for Additional Information on H*; RAI # 4; Model F and Model D5 Steam Generators," dated August 2009 (proprietary).

2. 1 copy of LTR-SGMP-09-109 NP-Attachment, "Response to NRC Request for Additional Information on H*; RAI # 4; Model F and Model D5 Steam Generators," dated August 2009 (non-proprietary).

Also enclosed is Westinghouse authorization letter CAW-09-2664 with accompanying affidavit, Proprietary Information Notice, and Copyright Notice.

As Item 1 contains information proprietary to Westinghouse Electric Company LLC, it is supported by an affidavit signed by Westinghouse, the owner of the information. The affidavit sets forth the basis on which the information may be withheld from public disclosure by the Commission and addresses with specificity the considerations listed in paragraph (b)(4) of Section 2.390 of the Commission's regulations.

Accordingly, it is respectfully requested that the information which is proprietary to Westinghouse be withheld from public disclosure in accordance with 10 CFR Section 2.390 of the Commission's regulations.

Correspondence with respect to the copyright or proprietary aspects of the items listed above or the supporting Westinghouse affidavit should reference CAW-09-2664 and should be addressed to J. A. Gresham, Manager, Regulatory Compliance and Plant Licensing, Westinghouse Electric Company LLC, P.O. Box 355, Pittsburgh, Pennsylvania 15230-0355.